Bimonthly Report No. 6

November 2, 1963 to January 2, 1964

5549-6-P

STUDY AND INVESTIGATION OF A UHF-VHF ANTENNA

by

J. E. Herman
S. B. Rhee

Approved by John A. M. Lyon
John A. M. Lyon

COOLEY ELECTRONICS LABORATORY

Department of Electrical Engineering
The University of Michigan
Ann Arbor

5549-6-P = RL-2130

United States Air Force
Air Force Systems Command
Aeronautical Systems Division
Contract No. AF 33(657)-10607
Wright-Patterson Air Force Base, Ohio

March 1964

TABLE OF CONTENTS

	Page
LIST OF ILLUSTRATIONS	iii
ABSTRACT	iv
1. REPORTS, TRAVEL, AND VISITORS	1
2. PERIOD ACTIVITIES	1
2.1 Ferrite Loaded Rectangular Slot Antenna	1
2.1.1 Optimization of Ferrite Filled Rectangular Slot Antennas	1
2.1.2 Ferrite Loaded Rectangular Slot Antenna With Iris	10
2.2 Log Conical Spiral Antennas	10
2.2.1 Large Log Conical Spiral	11
2.2.2 Small Log Conical Spiral	11
2.3 Equiangular Spiral Antenna	13
2.4 Log Spiral Zig-Zag Antenna	20
3. FUTURE RESEARCH EFFORT	21
3.1 Equiangular Spiral Antenna	21
3.2 Log Zig-Zag Antenna	21
3.3 Log Conical Spiral Antenna	21
3.4 Magnetic Tuning	21
4. SUMMARY AND CONCLUSIONS	24
APPENDIX A: Radiation Patterns for the Small Log Conical Spiral Antenna	26
APPENDIX B: Radiation Patterns for the Large Log Conical Spiral Antenna	39

LIST OF ILLUSTRATIONS

Figure		Page
1.	$\|T\|^2$ and bandwidth as a function of μ_r; for all points, $\mu_r t_r = 9$, b/a = .3, $F_N = 1.8$. (a) Tendency for efficiency to have a maximum. (b) Tendency for bandwidth to have a maximum.	4
2.	Peaking of radiation efficiency (Aperture transmission coefficient squared).	7
3.	Dependence of μ_r (optimum) on $\mu_r\epsilon_r$ product and physical dimensions of slot ($ka/\pi = 1.9$).	8
4.	Ferrite loading for the large, log conical spiral antenna. (a) Loading with a thin uniform layer, type A material. (b) Loading with a tapered thick layer, type B material. (c) Loading with a uniform thin layer on the bottom half. (d) Loading with a uniform thick layer on the bottom half.	12
5.	Ferrite loadings for the small log conical spiral antenna in a cavity.	14
6.	Frequency vs. VSWR for the small log conical spiral in a cavity.	15
7.	Spiral coordinates.	16
8.	Log spiral zigzag antenna, construction details.	22
9.	Frequency vs. VSWR for the log spiral zigzag antenna.	23
A-1 to A-12	Radiation Patterns for the Small Log Conical Spiral Antenna	27-38
B-1 to B-16	Radiation Patterns for the Large Log Conical Spiral Antenna	40-55

ABSTRACT

Design criteria for optimal use of ferrites in rectantular slot radiators have been established. Analysis firmly indicates that similar optimization can be achieved for annular slot antennas. Further experiments with log conical spirals have been performed which resulted in extension of frequency range. A log conical antenna taking full advantage of the frequency range of the available ferrite powder has been made. Final test results on this design will be available shortly. The thickness of ferrite surrounding log conical antenna elements appears to be a negligible factor. An analytical study of the equiangular spiral which can be adapted to the introduction of layers of ferrite has been completed. Computer results for specific cases are not yet available. Preliminary test data on a log zig-zag antenna using powdered ferrite are presented.

1. REPORTS, TRAVEL, AND VISITORS

None

2. PERIOD ACTIVITIES

2.1 Ferrite Loaded Rectangular Slot Antenna

Further deductions and implications have been made concerning the utilization of ferrite material in rectangular slot antennas. Systematic procedures have been obtained which enable the optimum use of the ferrite material for the purpose of improving the efficiency of the antenna or increasing the effective aperture area for a given physical aperture size. Further preliminary analysis indicates that the optimization design procedures can also be applied successfully to rectangular slot antennas.

2.1.1 Optimization of Ferrite Filled Rectangular Slot Antennas. Utilizing the variational procedures upon the electronic computer it has been apparent that the $\mu_r \epsilon_r$ product is a determining factor in many of the problems of interest. It therefore appears that an important design requirement is to establish the optimum μ_r value for a given $\mu_r \epsilon_r$ product and a given size of aperture. Another design consideration to be obtained is to establish the proper $\mu_r \epsilon_r$ product for a specific size of aperture. Finally, a third design requirement would be to establish the proper top-to-bottom dimension of a rectangular slot compared to the side-to-side dimension of the slot when the slot is

filled with ferrite material. It has been found that the radiation efficiency can be maximized by a specific value of μ_r occurring in a given $\mu_r\epsilon_r$ product when applied to a given aperture. The other two optimizations where mentioned above are not true maximum-minimum problems, but result in a monotonic type of variation in each case. However, the knowledge of the variation is helpful in the over-all design problem of such a rectangular antenna.

In further consideration of the process of optimizing the value of μ_r as mentioned for a given $\mu_r\epsilon_r$ product in a given aperture, use is made of a series of computations on a 7090 computer. Details of the variational analysis have been presented in prior Bimonthly Reports Nos. 1 and 2. Some experimental confirmation of the computer results are presented in Bimonthly Report No. 3. From the results in these reports, the fraction of the transmitted power for an infinite wave upon the aperture depends upon $|T|^2$. The design procedure is then to calculate the maximum value of $|T|^2$. Starting with the result of the previous reports there is the equation

$$\frac{1 - R}{1 + R} = \frac{Y}{Y_0} = G + jB \tag{1}$$

$$|T|^2 = 1 - |R|^2 = \frac{4G}{(1+G)^2 + B^2} \tag{2}$$

In Eq. 2 let K = G/B. Then for a given physical size of aperture, a

given $\mu_r \epsilon_r$ product and given frequency, K will be constant since G and B are proportional to μ_r.

$$|T|^2 = \frac{4KB}{(1-KB)^2 + B^2} \tag{3}$$

Equation 3 may now be differentiated with respect to B:

$$\frac{d|T|^2}{dB} = 0 \tag{4}$$

where

$$B = \sqrt{\frac{1}{1+k^2}} \tag{5}$$

From this last equation the maximum value of $|T|^2$ is obtained:

$$|T|^2 = \frac{2\sqrt{\frac{K^2}{1+K^2}}}{1+\sqrt{\frac{K^2}{1+K^2}}} \tag{6}$$

It can be seen from the last expression that the maximum value corresponds to a value of μ_r which makes $B = \sqrt{1/(1+k^2)}$.

Figure 1 shows a plot of $|T|^2$ and bandwidth as a function of μ_r for the following parametric values:

$$\mu_r \epsilon_r = 9$$

$$b/a = .3$$

$$F_N = 1.8$$

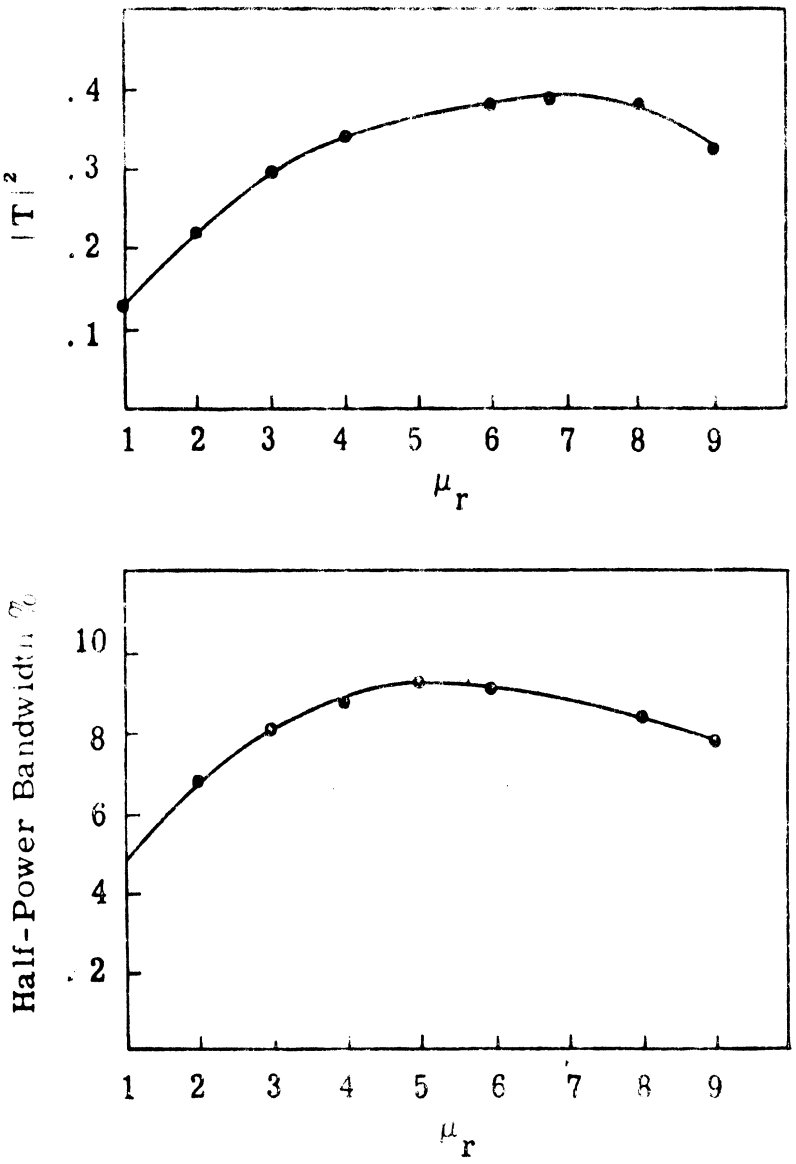

Fig. 1. $|T|^2$ and bandwidth as a function of μ_r; For all points $\mu_r t_r = 9$, $b/a = .3$, $F_N = 1.8$. (a) Tendency for efficiency to have a maximum. (b) Tendency for bandwidth to have a maximum.

It is to be noted that the maximum value of $|T|^2$ occurs at $\mu_r = 6.8$ and has been predicted by the equation for B above. However, the maximum value of bandwidth occurs for $\mu_r = 5.0$. The reason for this is that as μ_r increases the electrical length of the cavity increases. This effect tends to decrease bandwidth and leads for a bandwidth maximum at a value of μ_r slightly less than the μ_r value corresponding to maximum $|T|^2$. The same reasoning would apply to the problem of maximizing the efficiency since the increase in cavity length will increase the losses incurred. It is very interesting to note according to Fig. 1 the maximum bandwidth is almost double that obtainable for the pure dielectric case ($\mu_r = 1$, $\epsilon_r = 9$). This is supported by the experimental data shown in Table I for the dielectric cavity and powdered-ferrite filled cavity. These antennas are exactly the same size and operate at almost the same frequency.

Figure 2 summarizes the information on $|T|^2$ since it is a plot of $|T|^2$ versus B with K as a parameter. Every plot of $|T|^2$ versus μ_r such as shown in Fig. 1 will lie along one of the constant K curves. For a given aperture size, $\mu_r\epsilon_r$ product, and frequency, K can be determined from the variational data. Then as μ_r varies the constant K curves describe the variation of $|T|^2$ and B. Thus, the behavior of $|T|^2$ has a function of μ_r can be determined immediately from the curve of Fig. 2. Figure 3 shows the plot of optimum of μ_r as a function of the product $\mu_r\epsilon_r$ for $ka/\Pi = 1.9$. It is to be noted that the

Table 1

COMPARISON OF RECTANGULAR SLOT ANTENNAS

	Size	Volume (cu.in.)	BW with Flange VSWR = 3.0 (mc)	BW with Flange VSWR = 6.0 (mc)	BW-No Flange VSWR = 3.0 (mc)	BW-No Flange VSWR = 6.0 (mc)	Eff.	Dir. (deg)	Weight (lbs)
Air loaded	30" x 7½" x 10"	2250			64	90	90%	5.8	25.75
Power loaded	12" x 3" x 4"	144	22	50	20	36	65%	5.0	16.75
Solid loaded	5" x 2" x 1½"	15	19	34	19	32	30%	5.0	3.6
Dielectric loaded	12" x 3" x 4"	144	10	18	8	16	85%	5.0	14.5

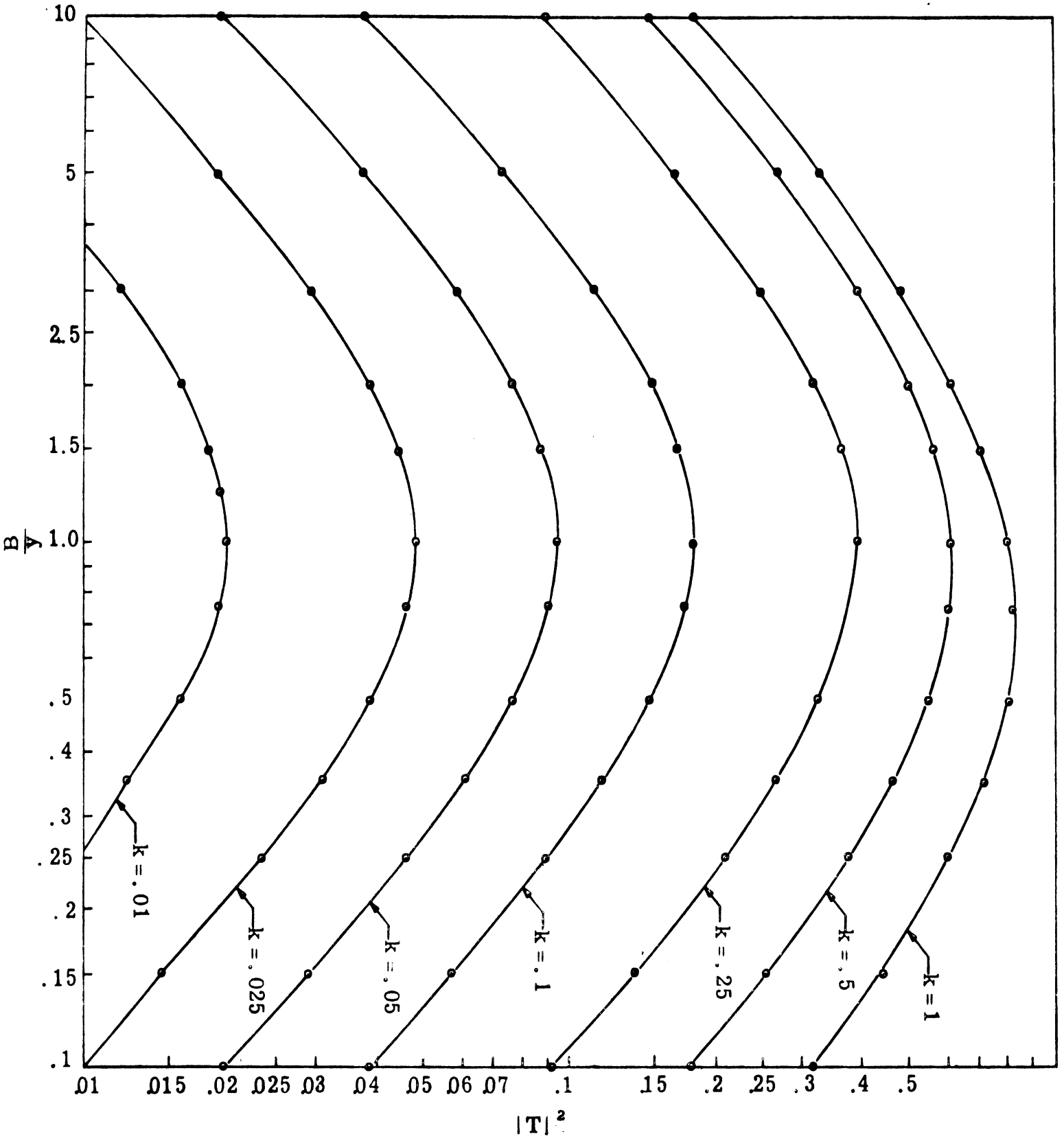

Fig. 2. Peaking of radiation efficiency (Aperture transmission coefficient squared).

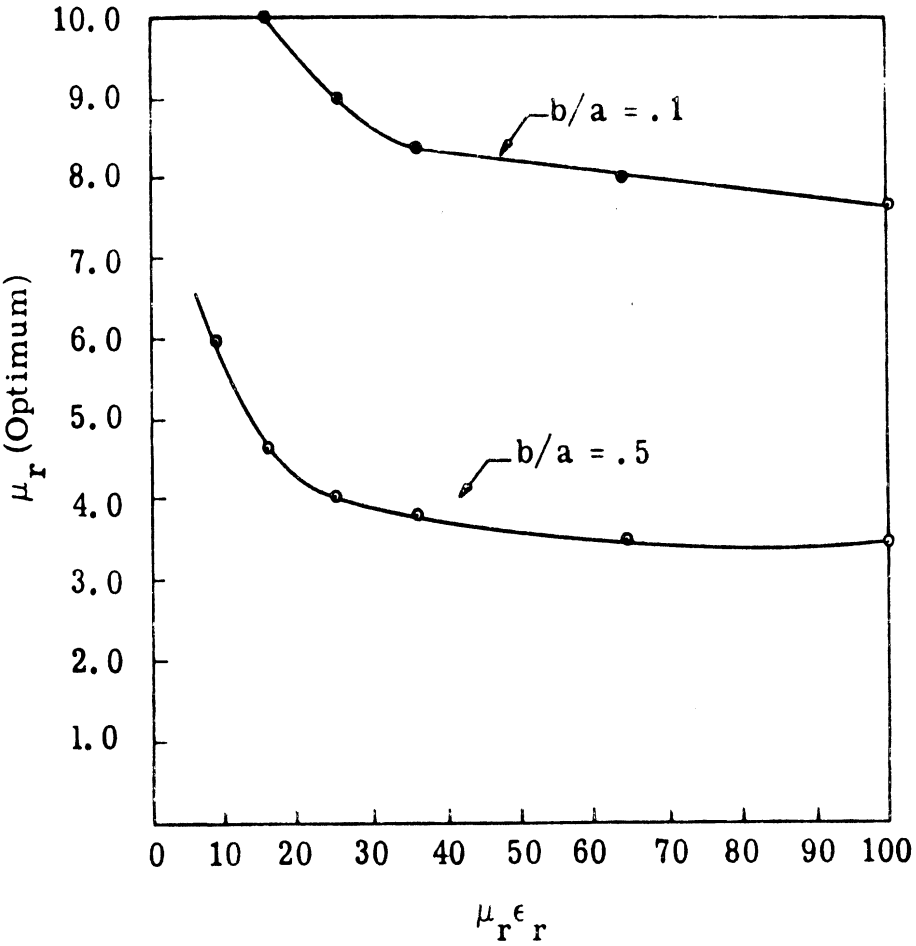

Fig. 3. Dependence of μ_r (optimum) on $\mu_r \epsilon_r$ product and physical dimensions of slot ($ka/\pi = 1.9$).

optimum value of μ_r decreases with increasing $\mu_r\epsilon_r$ product.

In consideration of the problem of the dependence of $\mu_r\epsilon_r$ on the physical size of the aperture, a check of the computed data for G and B reveals that for a given physical aperture size and frequency different values of $\mu_r\epsilon_r$ yield almost exactly the same values of K. This agrees with the asymptotic expression for 1/K or B/G. This asymptotic expression is valid for large values of $\mu_r\epsilon_r$.

$$\frac{B}{G} = \frac{1}{2\Pi} \times \left(\frac{a}{b}\right) \times \frac{F_1(\theta_1)}{(k_o a/\Pi)^3} \qquad (7)$$

This latter expression is independent of the $\mu_r\epsilon_r$ product and depends only on the free space electrical size of the aperture K. This implies that a further optimization would yield identical values of $|T|^2$. However, the bandwidth would depend not only on $|T|^2$ but also on the rate of change with frequency of the aperture admittance parameters B'_s, B_A, and G_A. B_A and G_A are proportional to $1/\sqrt{F_{N^2}-1}$ and change very rapidly with frequency near cut-off. The rate of change of B'_s with frequency is proportional to the bandwidth ratio plotted in Fig. 1. Thus all parameters change very rapidly near cut-off and bandwidth improves monotonically as cut-off frequency decreases by increasing the $\mu_r\epsilon_r$ product.

Considering the dependency of the two dimensions the top-to-bottom dimension "b" and the side-to-side dimension "a", it is

observed that K varies approximately as $(b/a)^{\frac{1}{2}}$. In addition, the maximum value of T^2 approaches 2K for small values of K. Thus, the $|T|^2$ which was found to be roughly proportional to bandwidth and frequency has now been found to depend upon $(b/a)^{\frac{1}{2}}$ indicating that the dependents upon the "b" is not very pronounced since it is a square root dependency.

2.1.2 Ferrite Loaded Rectangular Slot Antenna With Iris.

A further study of appropriate design procedures for maximizing the performance of a rectangular slot antenna using an iris in the aperture plane has been made. The details of the validation of the design procedures are to be found in the final report on rectangular slot antennas utilizing ferrite which is in preparation. However, in the case of slots having irises, the effect of an increase with μ_r is to increase the length of the cavity and the optimum efficiency and bandwidth values occur at slightly lower values of μ_r.

2.2 Log Conical Spiral Antennas

As a continuation of the work of the previous period, several different types of ferrite powder loading and their effects on pattern and voltage standing wave ratio (VSWR) were studied. The studies were carried out on the same log conical spiral antennas used previously.

Two types of ferrite powders were used during this period and were designated types "A" and "B". Type A powder has the best magnetic Q over the frequency range 100-900 Mc but only a limited

quantity is available. Type B powder is of inferior quality but is available in quantity and was used for preliminary tests where radiation efficiency was not a prime consideration. This was acceptable for studies of the effects of loading on the radiation patterns of the antennas.

2.2.1 Large Log Conical Spiral. Results obtained by loading the antenna with a thin uniform layer of type A material were reported in BMR No. 5 [Fig. 4(a)]. During this period, type B powder was used to form a tapered thick layer [Fig. 4(b)], a uniform thin layer on the bottom half of the antenna [Fig. 4(c)], and a uniform thick layer on the bottom half of the antenna [Fig. 4(d)].

For each type of loading, radiation patterns were taken for E_θ and E_ϕ at frequencies of 350 Mc, 500 Mc, 700 Mc, and 900 Mc. These are shown in Appendix B.

The dimensions of the antenna are as follows:

Base diameter	17.5 cm
Apex diameter	5.0 cm
Height	47.0 cm
Apex angle	15°
Pitch angle	73°

2.2.2 Small Log Conical Spiral. This antenna was designed according to Dyson's[1] design data. The dimensions are as follows:

Base diameter	13.0 cm
Apex diameter	6.0 cm
Height	30.0 cm
Apex angle	10°
Pitch angle	73°

---

[1] John D. Dyson, "The Unidirectional Equiangular Spiral Antenna," IRE Transactions on Antenna and Propagation, October 1959, p. 329.

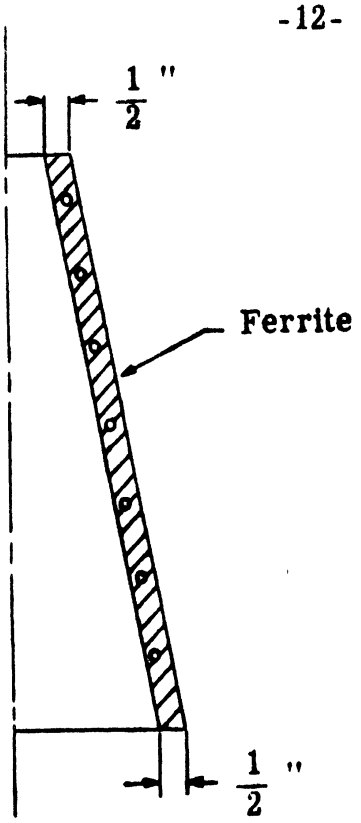

Fig. 4a
Loading with a thin uniform layer, type A material.

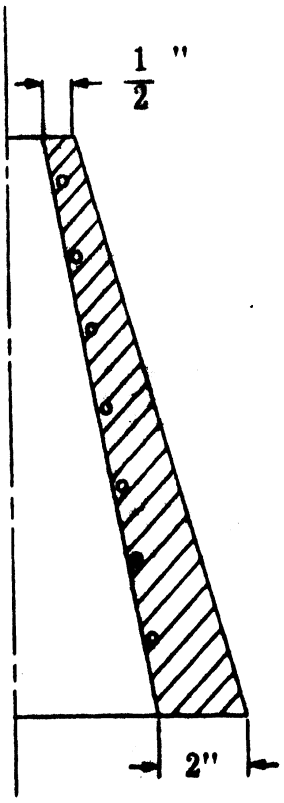

Fig. 4b
Loading with a tapered thick layer, type B material.

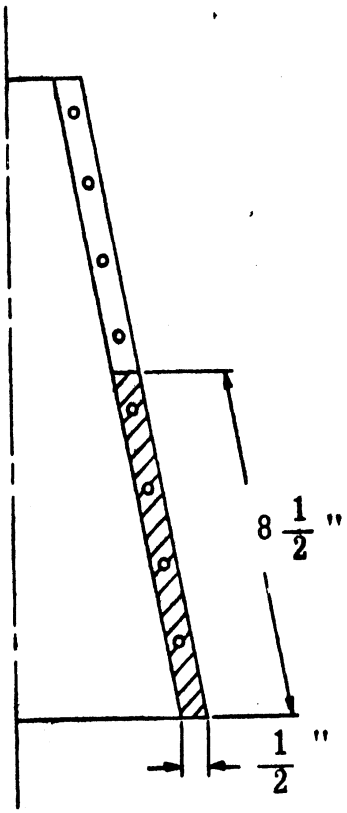

Fig. 4c
Loading with a uniform thin layer on the bottom half.

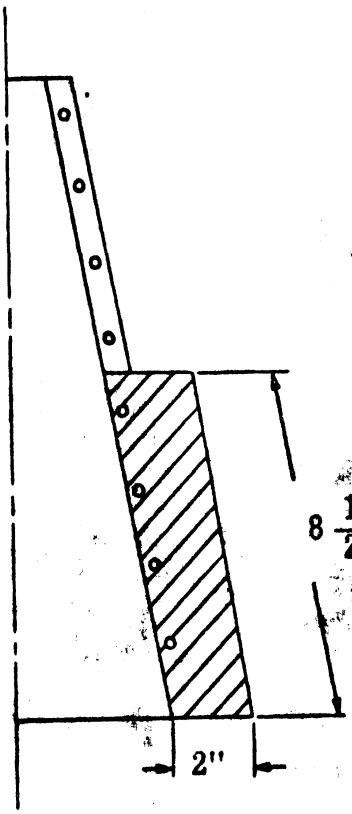

Fig. 4d
Loading with a uniform thick layer on the bottom half.

Fig. 4. Ferrite loading for the large log conical spiral antenna.

An aluminum cylindrical cavity was made to adapt the conical spiral to flush-mounted operation.

Several different types of loading with type A powder are shown schematically in Figs. 5(a) - 5(d). Radiation patterns for each loading were taken for E_θ and E_ϕ at frequencies of 500 Mc, 700 Mc, and 900 Mc. These are shown in Appendix A. Figure 6 shows frequency versus VSWR for the various types of loading for the small log conical spiral.

2.3 Equiangular Spiral Antenna

During the period a mathematical expression for the radiation fields of the equiangular spiral thin-wire (or slot) antenna was found. This expression is adaptable to solution using the IBM 7090 computer if the current distribution and mode of excitation are specified.

Consider the planar monofilar spiral shown in Fig. 7, where (r', ϕ') are source coordinates, (r, θ, ϕ) are field coordinates, and $r'' = |\underline{r} - \underline{r}'|$. The magnetic vector potential for a thin current distribution in space is

$$\underline{A}^{(1)}(r, \theta, \phi) = \frac{\mu_0}{4\pi} \int_{\text{spiral}} \frac{\underline{I}(1')\, e^{jkr''}}{r''}\, dl' \qquad (8)$$

where the $e^{-j\omega t}$ time dependence is understood. In the radiation field phase variations are taken into account by

$$r'' = r - r' \sin\theta \cos(\phi - \phi') . \qquad (9)$$

The equation of the equiangular spiral is

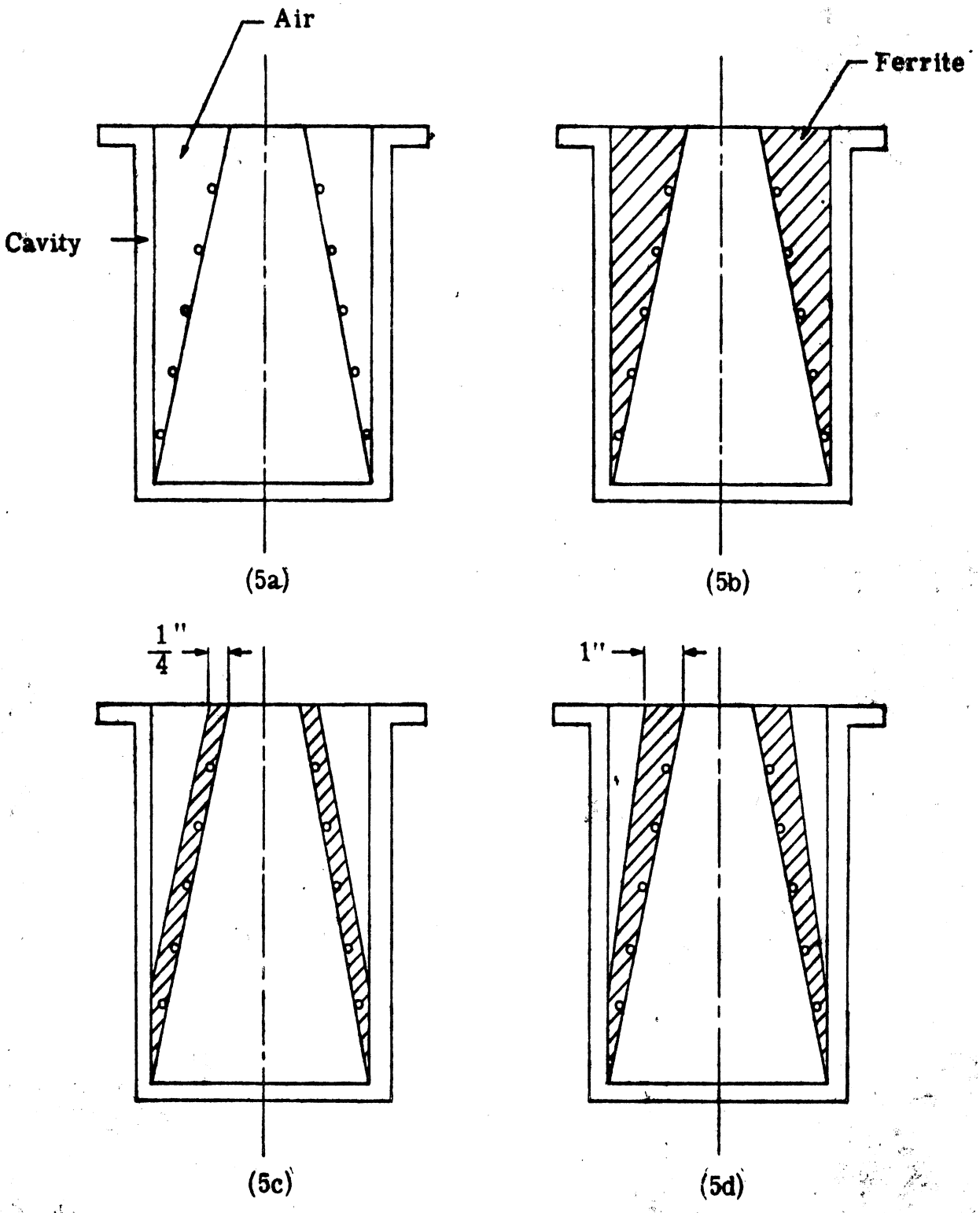

Fig 5. Ferrite loading for small log conical spiral antenna in a cavity.

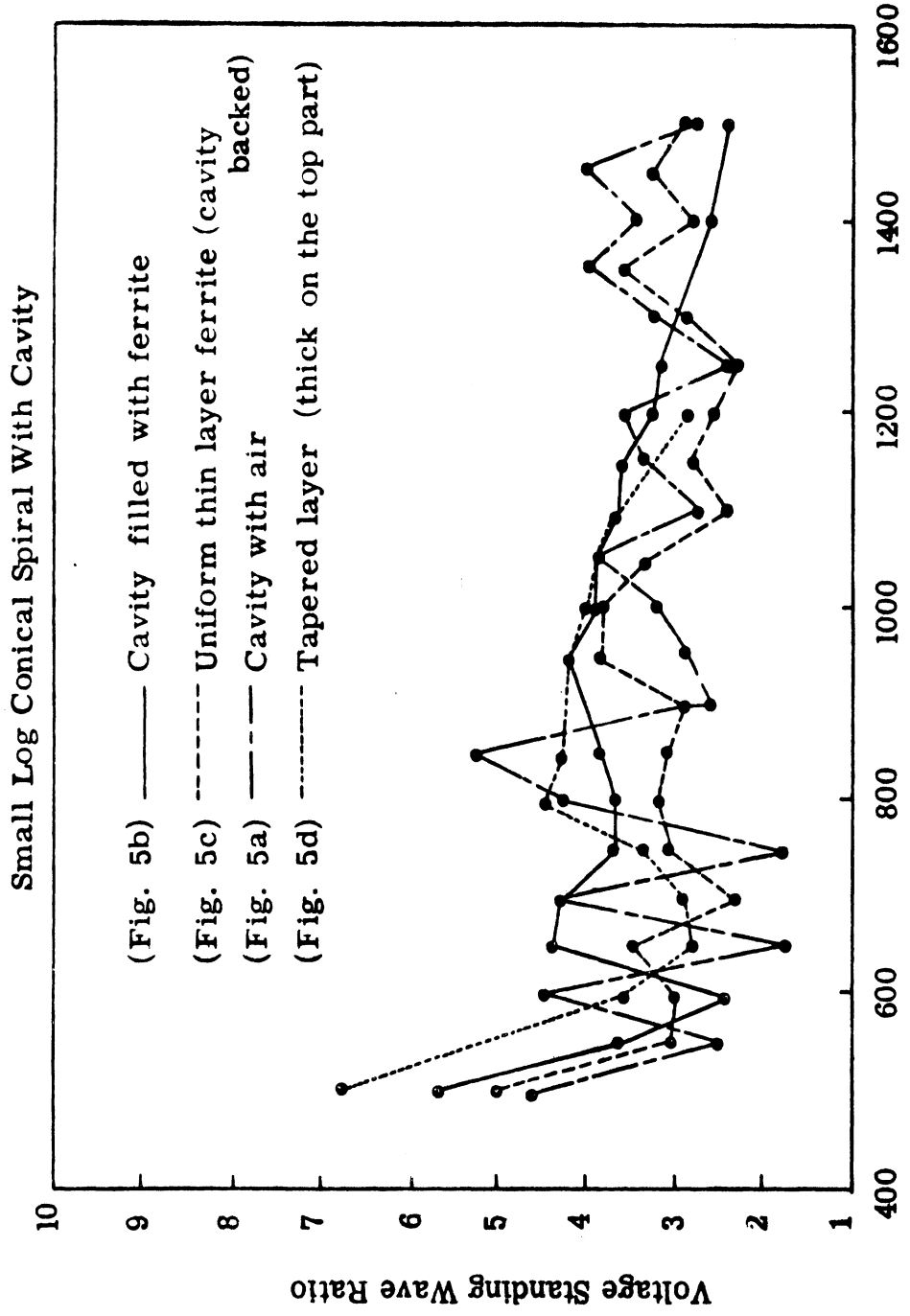

Fig. 6. Frequency versus VSWR for the small log conical spiral with cavity.

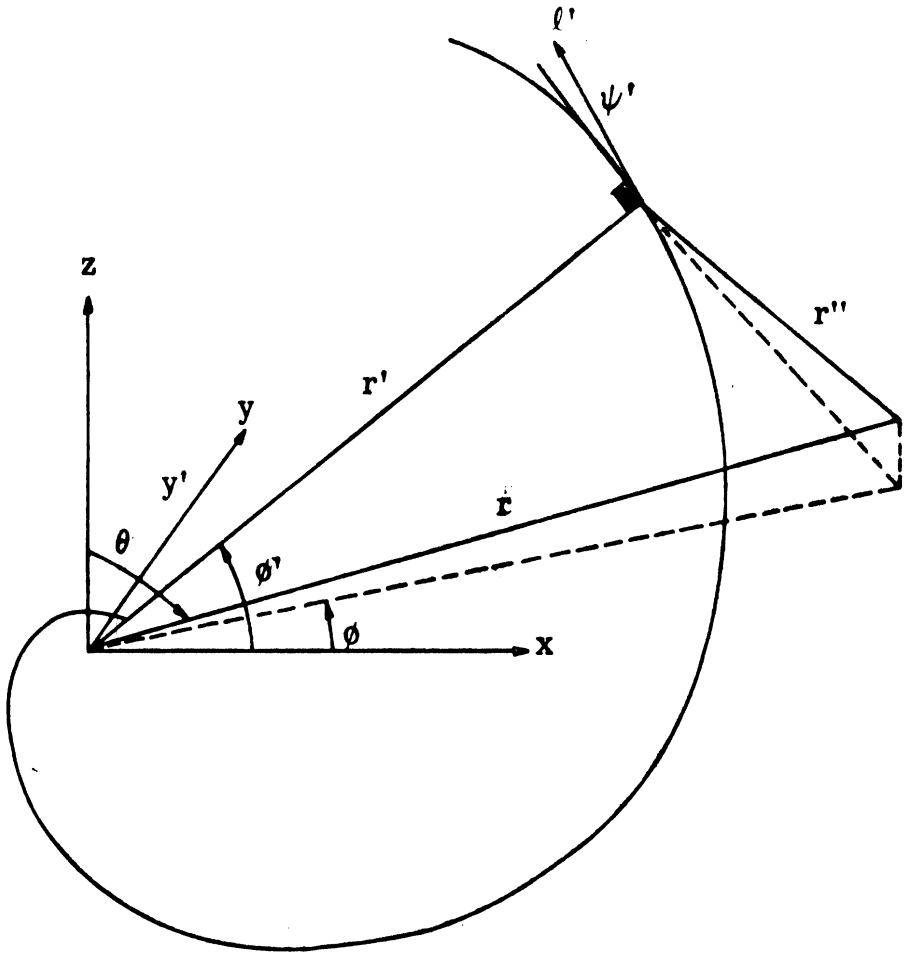

Fig. 7. Spiral coordinates

$$r' = r'_0 e^{a\phi'} \tag{10}$$

whence

$$d\ell' = \sqrt{(dr')^2 + (r'd\phi')^2} = \sqrt{1+a^2}\; r'_0 e^{a\phi'} d\phi' \tag{11}$$

and

$$\ell' = \int_0^{\phi'} d\ell' = \sqrt{1 + \frac{1}{a^2}}\; r'_0 (e^{a\phi'} - 1) . \tag{12}$$

The direction of the segment $d\ell'$ as shown in Fig. 7 is given by

$$\hat{\ell}' = \sin(\psi' - \phi') \hat{x} + \cos(\psi' - \phi') \hat{y} \tag{13}$$

where

$$\tan\psi' = \frac{dr'}{r'd\phi'} = a . \tag{14}$$

Since it is reasonable to assume the antenna impedance satisfies a variational expression, a zero order approximation to the current distribution may be made with only a second order error in the results. The zero order approximation to the current is that of a curved two-wire transmission line with no coupling to surrounding elements. This gives a current depending only on the distance (ℓ') along the line from the feed point, i.e., a traveling wave,

$$\underline{I}(\ell') = I_0 \left[e^{\gamma\ell'} + \Gamma e^{-\gamma\ell'}\right] \hat{\ell}'; \quad (\gamma = -\alpha + j\beta) \tag{15}$$

where ℓ' is given by (5) and Γ is the reflection coefficient. Thus the vector potential may be written as

$$\underline{A}^{(1)}(r,\theta,\phi) = \frac{\mu_o I_o}{4\pi}\,\frac{e^{jkr}}{r}\int_0^{\Phi}\left[e^{\gamma\ell'} + \Gamma e^{-\gamma\ell'}\right]\cdot$$

$$\cdot\left[e^{-jkr'_o}\,e^{a\phi'}\sin\theta\cos(\phi-\phi')\right]\cdot$$

$$\cdot\left[\sin(\psi'-\phi')\,\hat{x} + \cos(\psi'-\phi')\,\hat{y}\right]\cdot$$

$$\cdot\left[\sqrt{1+a^2}\;r'_o\,e^{a\phi'}\right]\,d\phi' \qquad (16)$$

For total reflection at the end of the wire the reflection coefficient becomes

$$\Gamma = -e^{2\gamma L};\quad\left(L = \sqrt{1+\frac{1}{a^2}}\;r'_o(e^{a\Phi}-1)\right) \qquad (17)$$

In spherical coordinates, the radiation field is related to the magnetic vector potential by

$$E_\theta = -j\omega A_\theta\;;\quad E_\phi = -j\omega A_\phi \qquad (18)$$

where

$$A_\theta = A_x\cos\theta\cos\phi + A_y\cos\theta\sin\phi$$

$$A_\phi = -A_x\sin\phi + A_y\cos\phi\,. \qquad (19)$$

Thus, if $\underline{A}$ is known the field can easily be found.

Consider the bifilar spiral with the currents in the two wires out of phase by an angle Δ at the feed. Then the total magnetic vector potential will be given by

$$\underline{A}(r,\theta,\phi,t) = \underline{A}^{(1)}(r,\theta,\phi,t) + \underline{A}^{(1)}(r,\theta,\phi+\pi,\ t+\frac{\Delta}{\omega}) \qquad (20)$$

Thus for balanced excitation ($\Delta = \pi$) the total magnetic vector potential is

$$\underline{A}(r,\theta,\phi) = -j\frac{\mu_o I_o}{2\pi}\sqrt{1+a^2}\ r'_o\ \frac{e^{jkr}}{r}\ e^{(\alpha - j\beta)\sqrt{1+\frac{1}{a^2}}\ r'_o} \cdot$$

$$\cdot \int_0^{\Phi} \left\{ \left[e^{(-\alpha+j\beta)\sqrt{1+\frac{1}{a^2}}\ r'_o\ e^{a\phi'}} - e^{(-\alpha+j\beta)\sqrt{1+\frac{1}{a^2}}\ r'_o(2e^{a\Phi} - e^{a\phi'})} \right] \right.$$

$$\cdot \cos\left[kr'_o \sin\theta \cos(\phi-\phi')\, e^{a\phi'}\right]\ e^{a\phi'} \cdot$$

$$\cdot \left[\sin(\psi'-\phi')\cos\phi + \cos(\psi'-\phi')\sin\phi\right]\cos\theta\ \hat{\theta} \cdot$$

$$\left. + \left[\cos(\psi'-\phi')\cos\phi - \sin(\psi'-\phi'\sin\phi\right]\ \hat{\phi} \right\}\ d\phi' . \qquad (21)$$

For convenience the following substitutions may be made:

$$z = a\phi'$$

$$z = a\Phi$$

$$\alpha' = \alpha\sqrt{1+\frac{1}{a^2}}\ r'_o$$

$$\beta' = \beta\sqrt{1+\frac{1}{a^2}}\ r'_o$$

$$k' = kr'_o$$

$$B = -j \frac{\mu_o I_o}{2\pi a} \sqrt{1 + a^2}\ r'_o \frac{e^{jkr}}{r} \qquad (22)$$

The pattern may be found for a $\phi = o$ or a $\phi = \pi$ cut. For the $\phi = o$ cut, Eq. 21 becomes

$$\underline{A}(r, \theta, o) = B\, e^{\alpha' l - j\beta'} \int_o^Z \left\{ \left[e^{(-\alpha' + j\beta')e^z} - e^{(-\alpha' + j\beta')(2e^z - e^z)} \right] \cdot \right. \qquad (23)$$

$$\left. \cdot \cos\left[k' \sin\theta \cos\frac{z}{a} e^z\right]\ e^z \left[\sin\left(\psi' - \frac{z}{a}\right) \cos\theta\ \hat{\theta} - \cos\left(\psi' - \frac{z}{a}\right) \hat{\phi}\right] \right\} dz$$

Equation 23 gives a set of integrals which may easily be evaluated by numerical methods on the computer. Whence, the magnitude and phase of the field components may be tabulated for each set of parameters.

The application of this method to a ferrite loaded antenna presents a difficult boundary value problem. However, it is hoped that a thin layer loading may be simulated by merely assuming the current propagates in a "slow-wave" mode, i.e., by assuming $\beta = \sqrt{\mu\epsilon}\ \ k$.

A computer program has been written and test data are being run. It is hoped that a full set of theoretical and experimental curves will be available for inclusion in the next bimonthly report.

2.4 Log Spiral Zig-Zag Antenna

A log zig-zag antenna was designed to take advantage of its reduced volume with frequency independent characteristics similar to

those of the log conical spiral. The dimensions used are shown in Fig. 8.

An initial test of the VSWR for a 1/4" thick uniform layer of type A powder was made and compared with the air loaded case (Fig. 9).

3. FUTURE RESEARCH EFFORT

3.1 Equiangular Spiral Antenna

A continuing effort will be made to obtain theoretical and experimental patterns of the equiangular spiral, including the case with a thin ferrite load.

3.2 Log Zig-Zag Antenna

During the next period, the effects of loading on beam pattern will be observed. Also a cavity will be constructed so that the antenna may be adapted to flush mounted operation.

3.3 Log Conical Spiral Antenna

A successful conclusion is anticipated for the experimental investigation of the log conical spiral. Investigation of the theoretical problem will continue.

3.4 Magnetic Tuning

A model of the solid ferrite-filled rectangular cavity-slot antenna delivered to WPAFB is currently being constructed for use in determining the effects of strong magnetic bias on the radiation properties

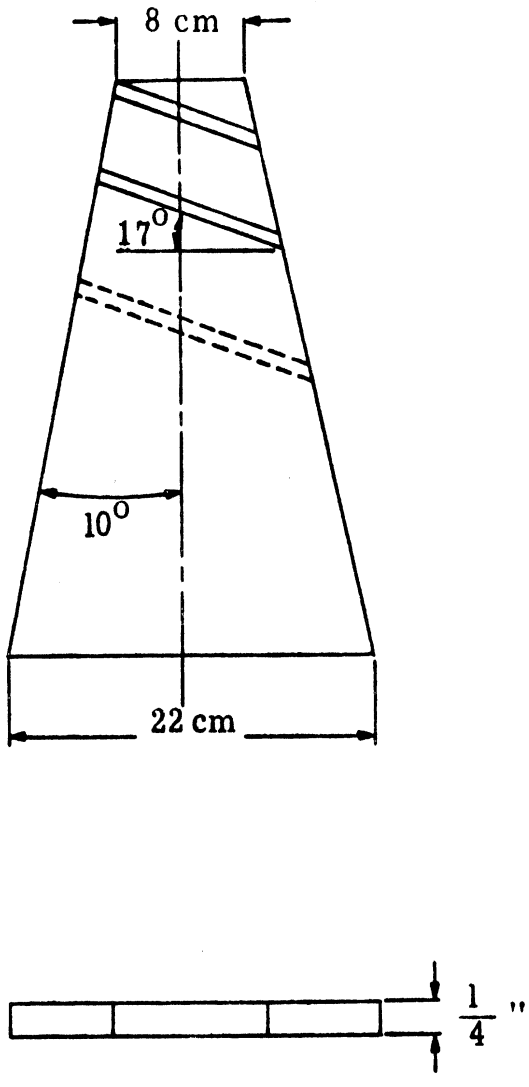

Fig. 8. Log spiral zigzag antenna construction details.

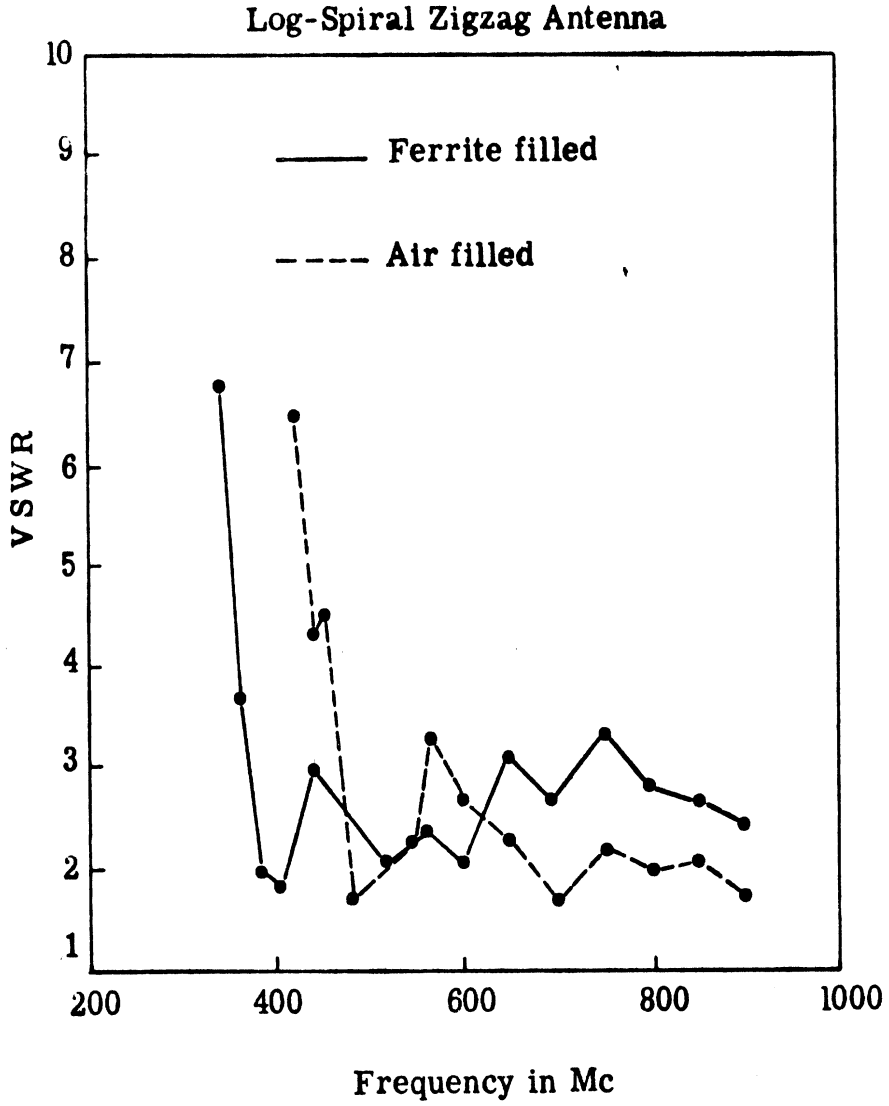

Fig. 9. Frequency versus VSWR for the log spiral zigzag antenna.

of the antenna. Preliminary measurements previously reported indicate that the resonant frequency of the cavity may be varied by introduction of a magnetic field across the antenna. This has the effect of varying the permeability of the ferrite material. In particular, the ferrite becomes anisotropic in the presence of a magnetic field.

4. SUMMARY AND CONCLUSIONS

A study of design procedures for ferrite-filled rectangular slot antennas has resulted in an optimal design requirement corresponding to the proper selection of the value of relative permeability for the highest radiation efficiency of the antenna. A further study of an available variational analysis of the annular slot antenna shows that the same optimization of radiating efficiency can be made for the annular slot using ferrite.

Best results on pattern, bandwidth, and radiation efficiency of a log conical spiral antenna can be obtained with a uniform loading of ferrite powder, although the thickness of the ferrite layers on each side of the conductor does not appear to be of great influence. So far major changes in radiation pattern have not been observed using ferrite. It is believed a more detailed analysis and testing program may show frequency regions where directivity increases and also frequency regions where this directivity may decrease. The latter is anticipated to some extent because of the miniaturization accomplished through the use of ferrite. Other workers have observed increased directivity of a helical

antenna using a hollow dielectric circular cylinder as a core.

Since, to date, only preliminary work performed loading of the equiangular spiral and the log zig-zag antenna, no conclusive results have been obtained.

APPENDIX A

RADIATION PATTERNS FOR THE SMALL LOG CONICAL SPIRAL ANTENNA

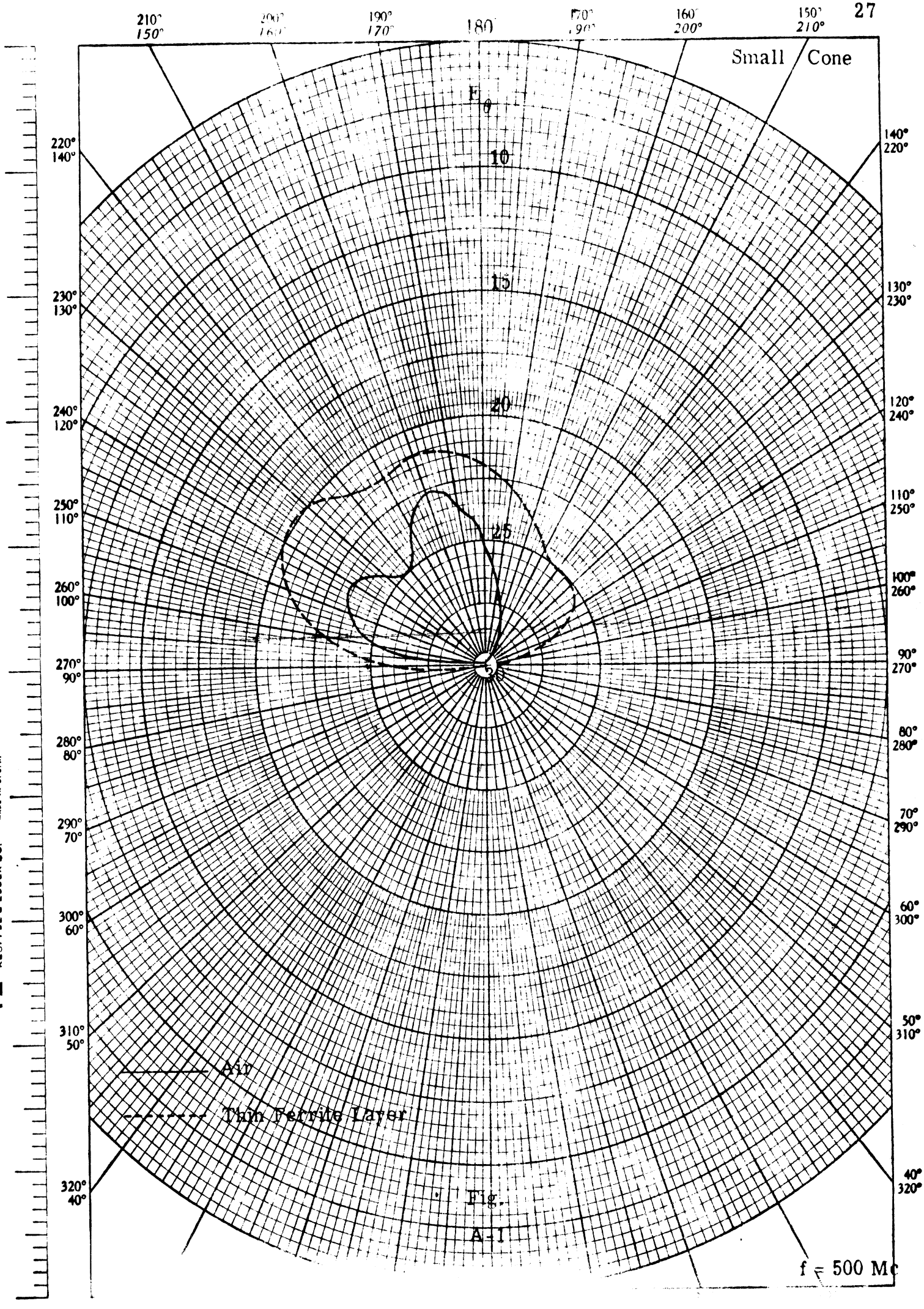
Small Cone
F_θ
10
15
20
25
Air
Thin Ferrite Layer
f = 500 Mc
K+E POLAR CO-ORDINATE 359-31
KEUFFEL & ESSER CO. MADE IN U.S.A.

Fig. A-1

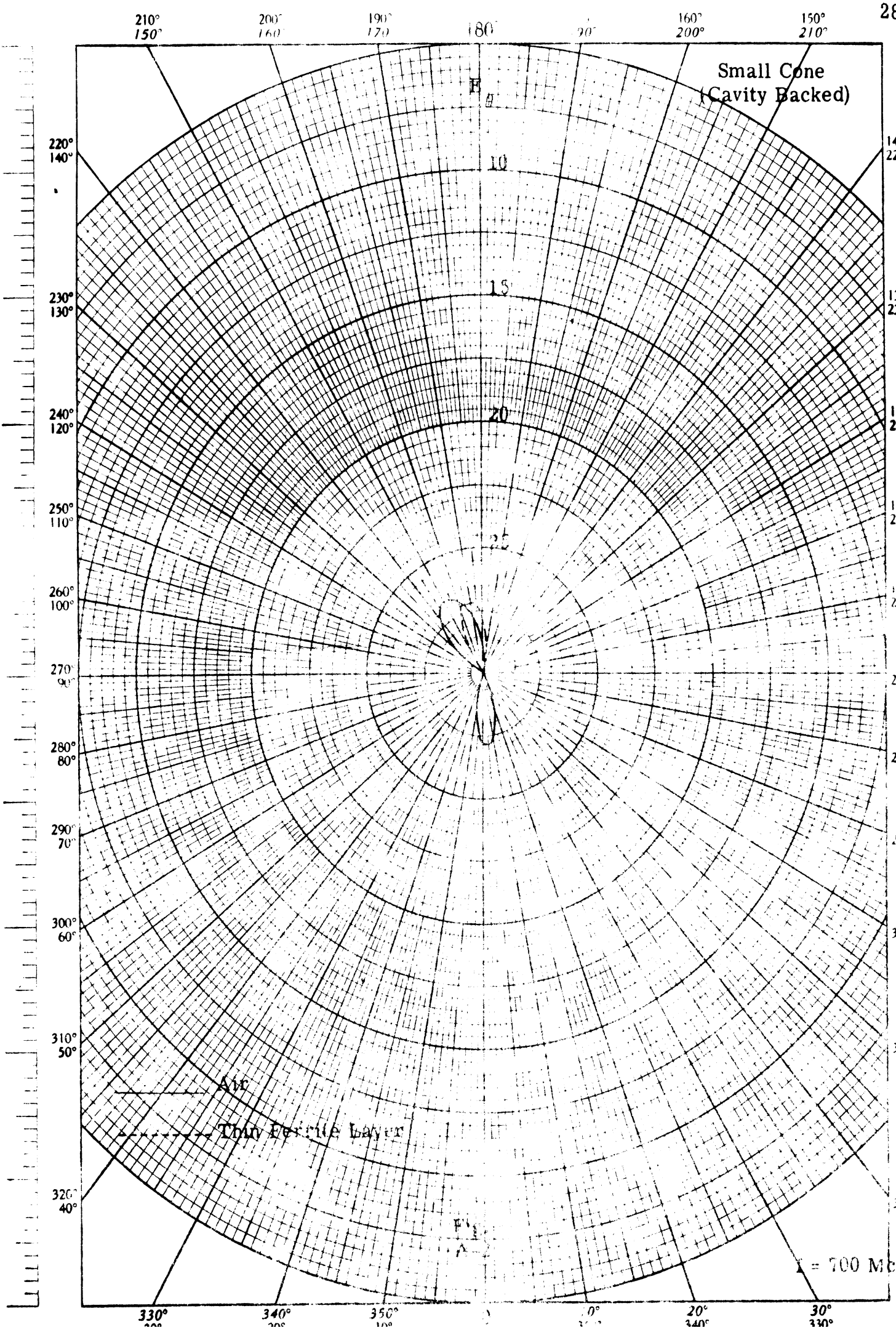
Small Cone
(Cavity Backed)
Air
Thin Ferrite Layer
f = 700 Mc
10
15
20
25
210° 150°
200° 160°
190° 170°
180°
160° 200°
150° 210°
220° 140°
230° 130°
240° 120°
250° 110°
260° 100°
270° 90°
280° 80°
290° 70°
300° 60°
310° 50°
320° 40°
330°
340°
350°
20°
30°
140° 220°
130° 230°
120° 240°
110° 250°
90° 270°
70°
60° 300°
50° 310°
40° 320°
KE POLAR CO-ORDINATE 359-31
KEUFFEL & ESSER CO

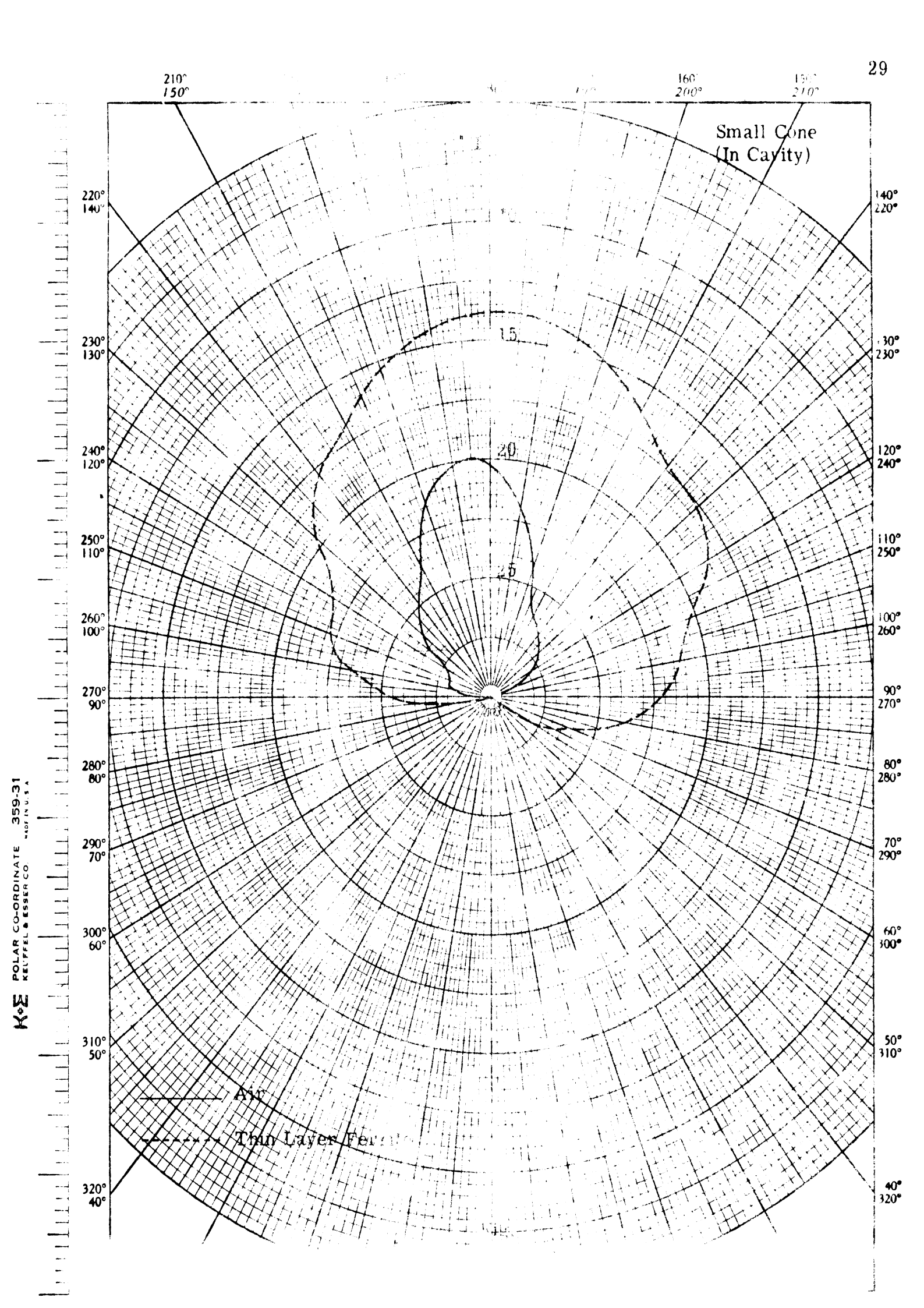
Small Cone
(In Cavity)
Air
Thin Layer Fer
POLAR CO-ORDINATE 359-31
KEUFFEL & ESSER CO. MADE IN U.S.A.

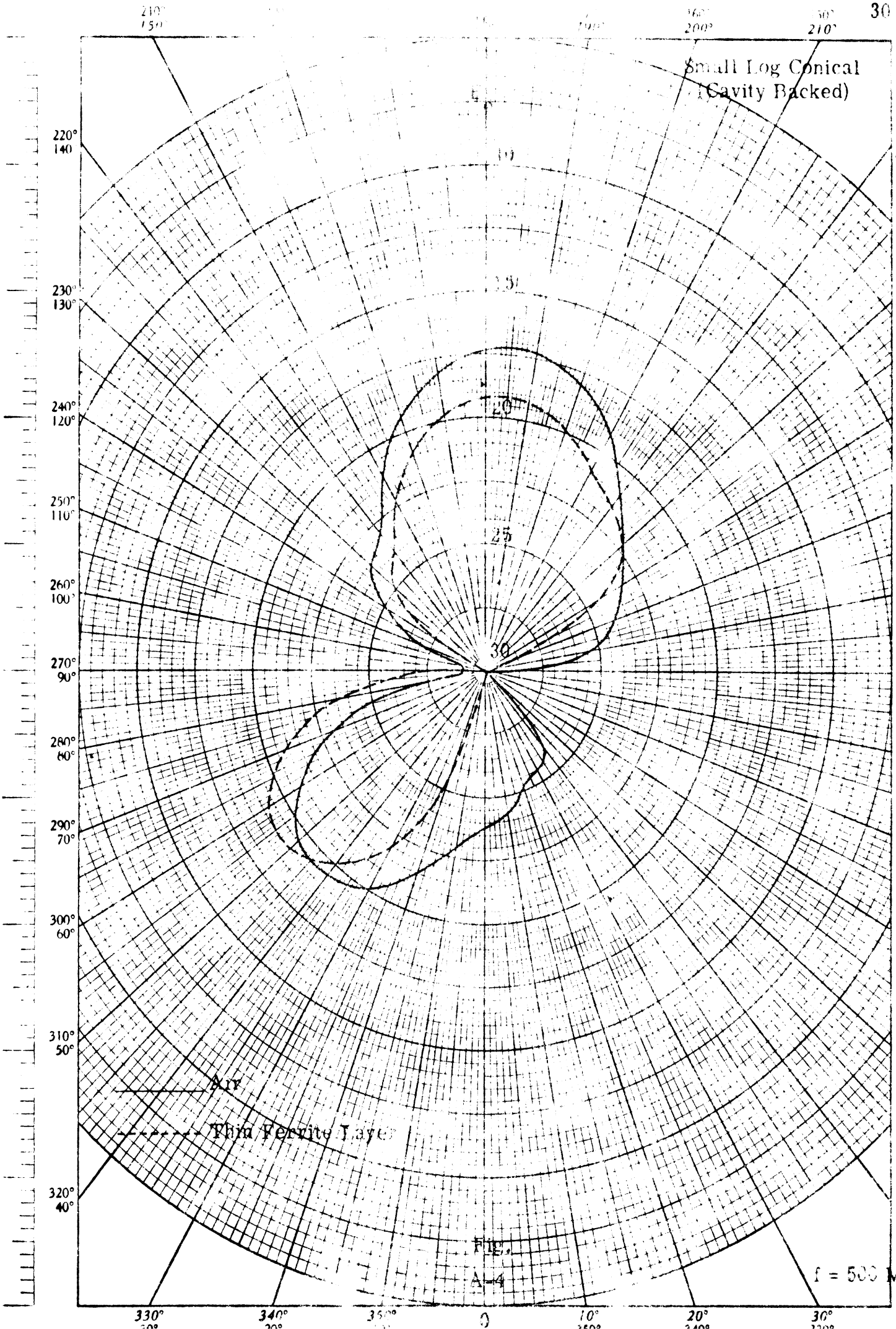
Small Log Conical
(Cavity Backed)
Air
Thin Ferrite Layer
f = 500 Mc

Fig. A-4

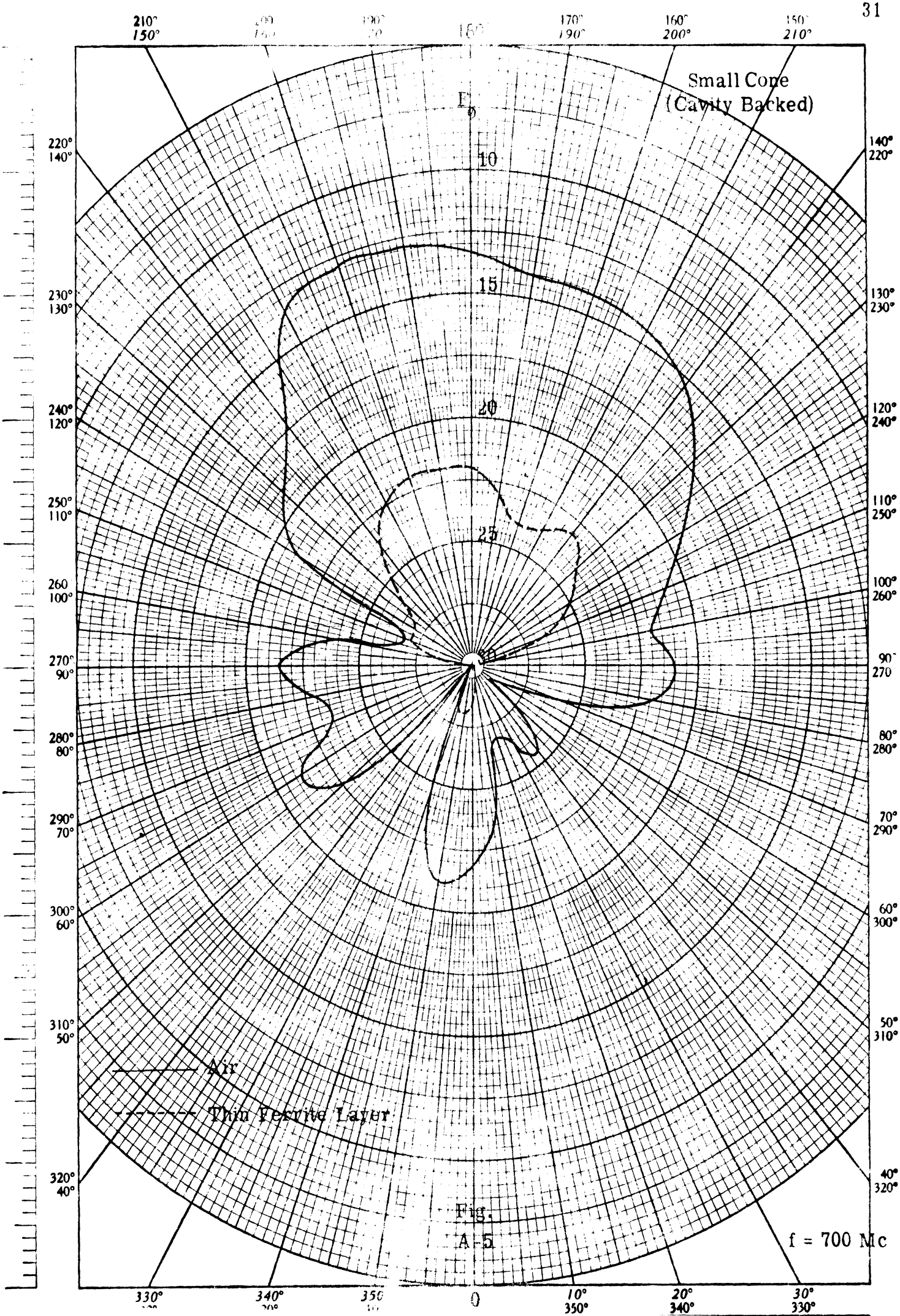
Small Cone
(Cavity Backed)
E
θ
10
15
20
25
Air
Thin Ferrite Layer
f = 700 Mc
210° 150°
200° 160°
190° 170°
180°
170° 190°
160° 200°
150° 210°
140° 220°
130° 230°
120° 240°
110° 250°
100° 260°
90° 270°
80° 280°
70° 290°
60° 300°
50° 310°
40° 320°
330° 30°
340° 20°
350° 10°
0
K&E POLAR CO-ORDINATE 359-31
KEUFFEL & ESSER CO.

Fig. A-5

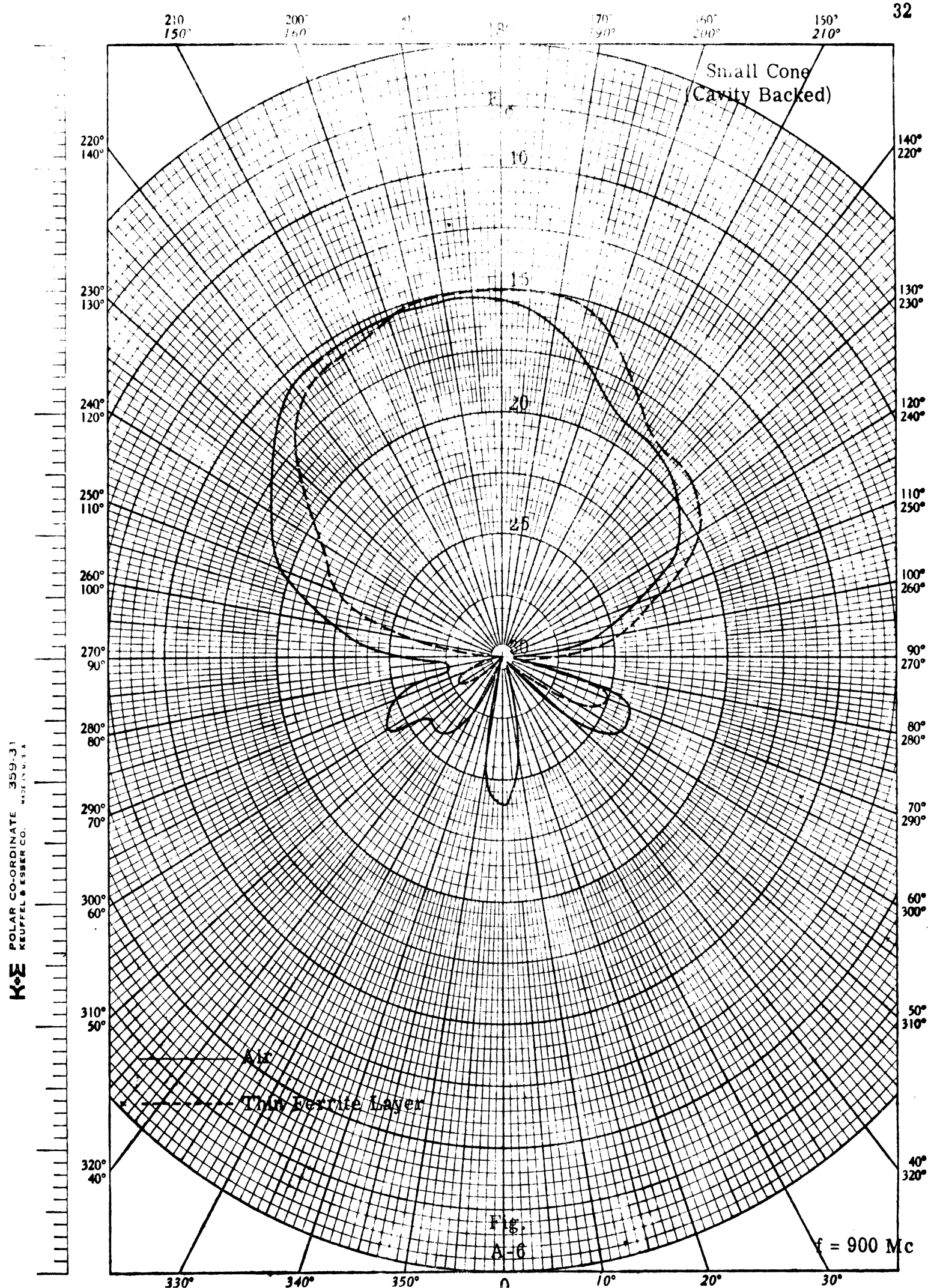

Fig. A-6

K&E POLAR CO-ORDINATE 359-31
KEUFFEL & ESSER CO. MADE IN U.S.A.

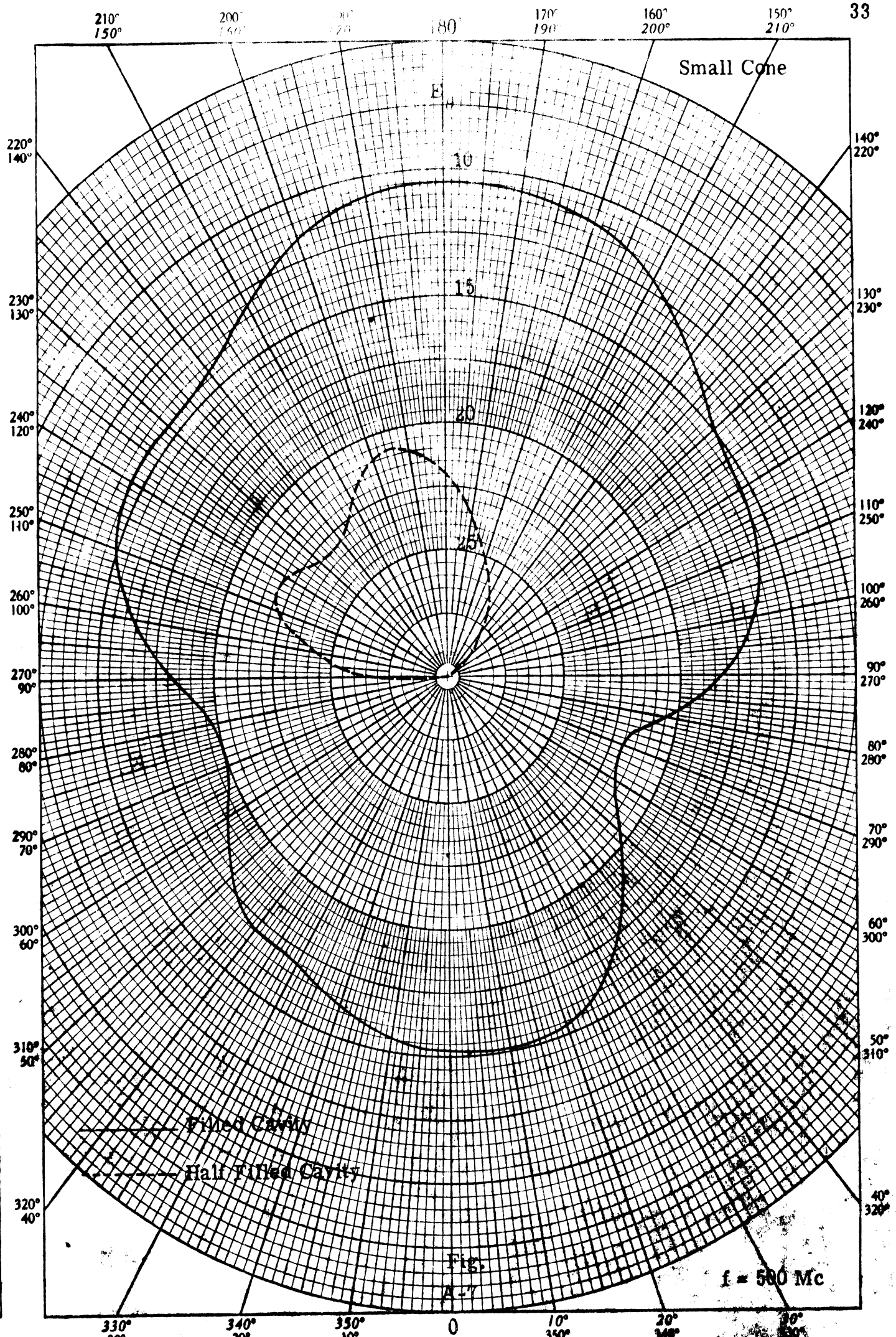
Small Cone
E
10
15
20
25
210° 150°
200° 160°
180°
170° 190°
160° 200°
150° 210°
220° 140°
230° 130°
240° 120°
250° 110°
260° 100°
270° 90°
280° 80°
290° 70°
300° 60°
310° 50°
320° 40°
140° 220°
130° 230°
120° 240°
110° 250°
100° 260°
90° 270°
80° 280°
70° 290°
60° 300°
50° 310°
40° 320°
330° 30°
340° 20°
350° 10°
0
10° 350°
20° 340°
30° 330°
Filled Cavity
Half Filled Cavity
f = 500 Mc

Fig. A-7

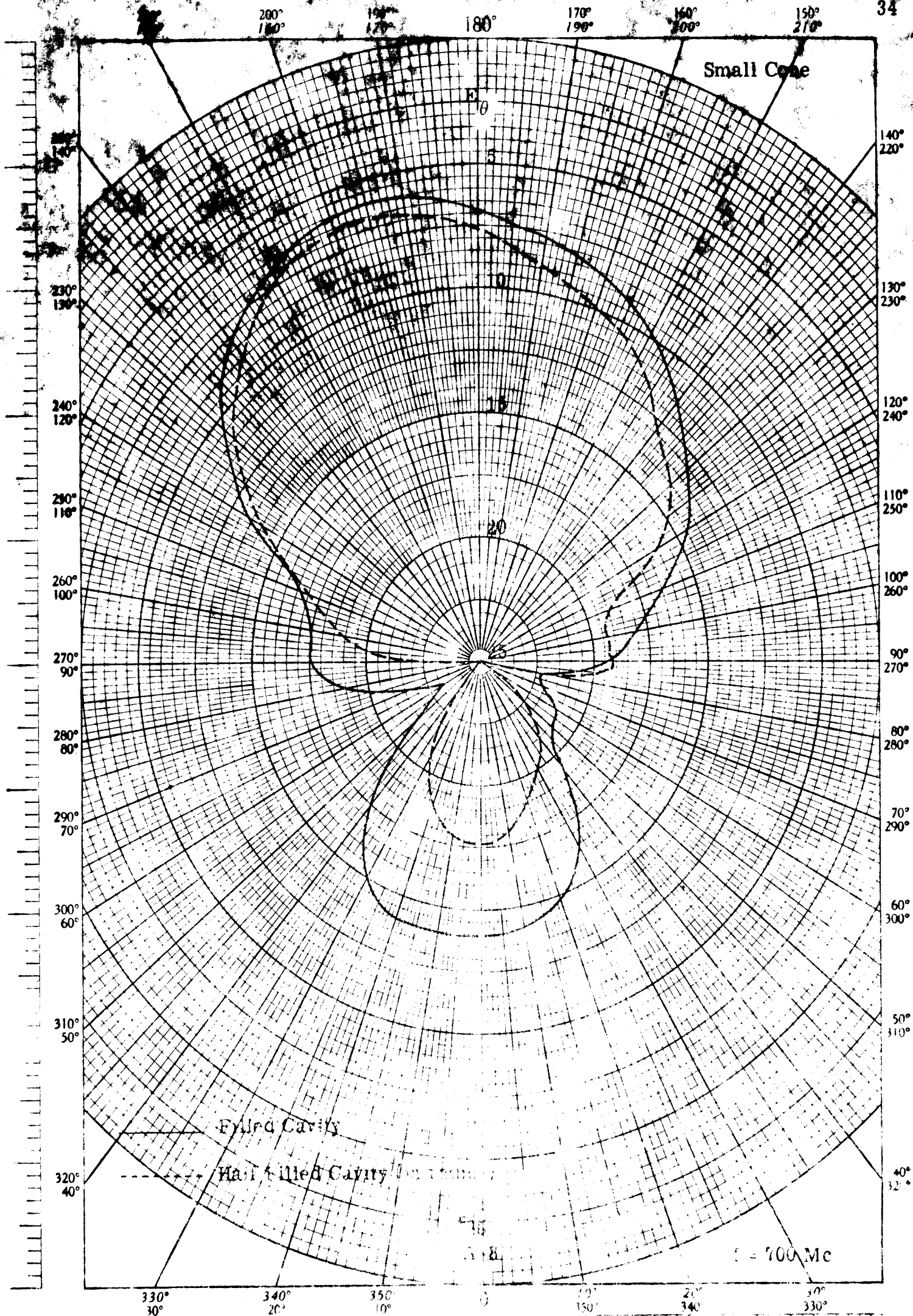
Small Cone
E_θ
180°
5
10
15
20
25
Filled Cavity
Half Filled Cavity
f = 700 Mc

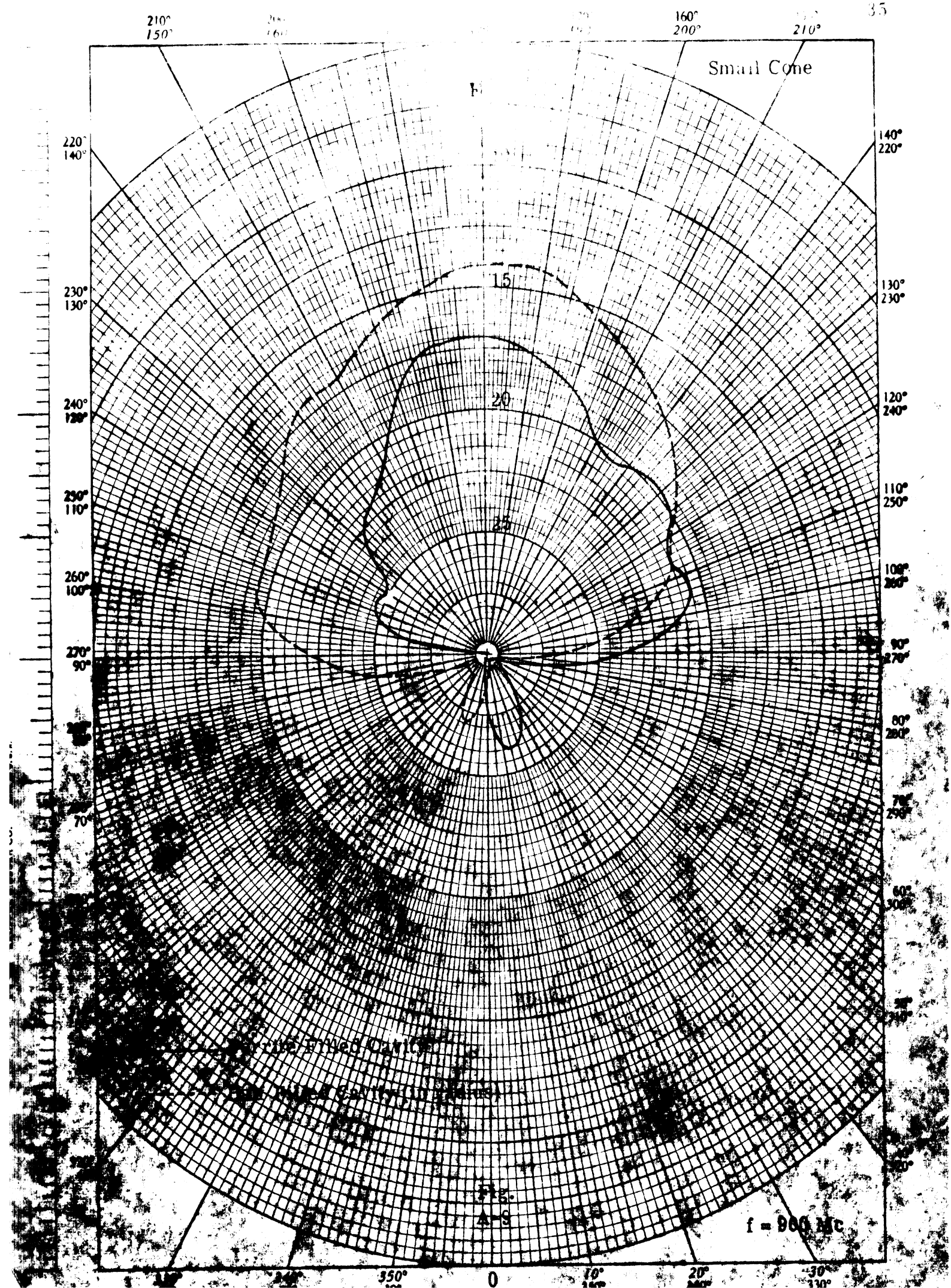
Small Cone
210°
150°
160°
200°
210°
220°
140°
140°
220°
230°
130°
130°
230°
240°
120°
120°
240°
250°
110°
110°
250°
260°
100°
100°
260°
270°
90°
90°
270°
80°
280°
70°
290°
60°
300°
15
20
25
Fig.
A-9
f = 900 Mc
350°
0
10°
20°
30°
330°

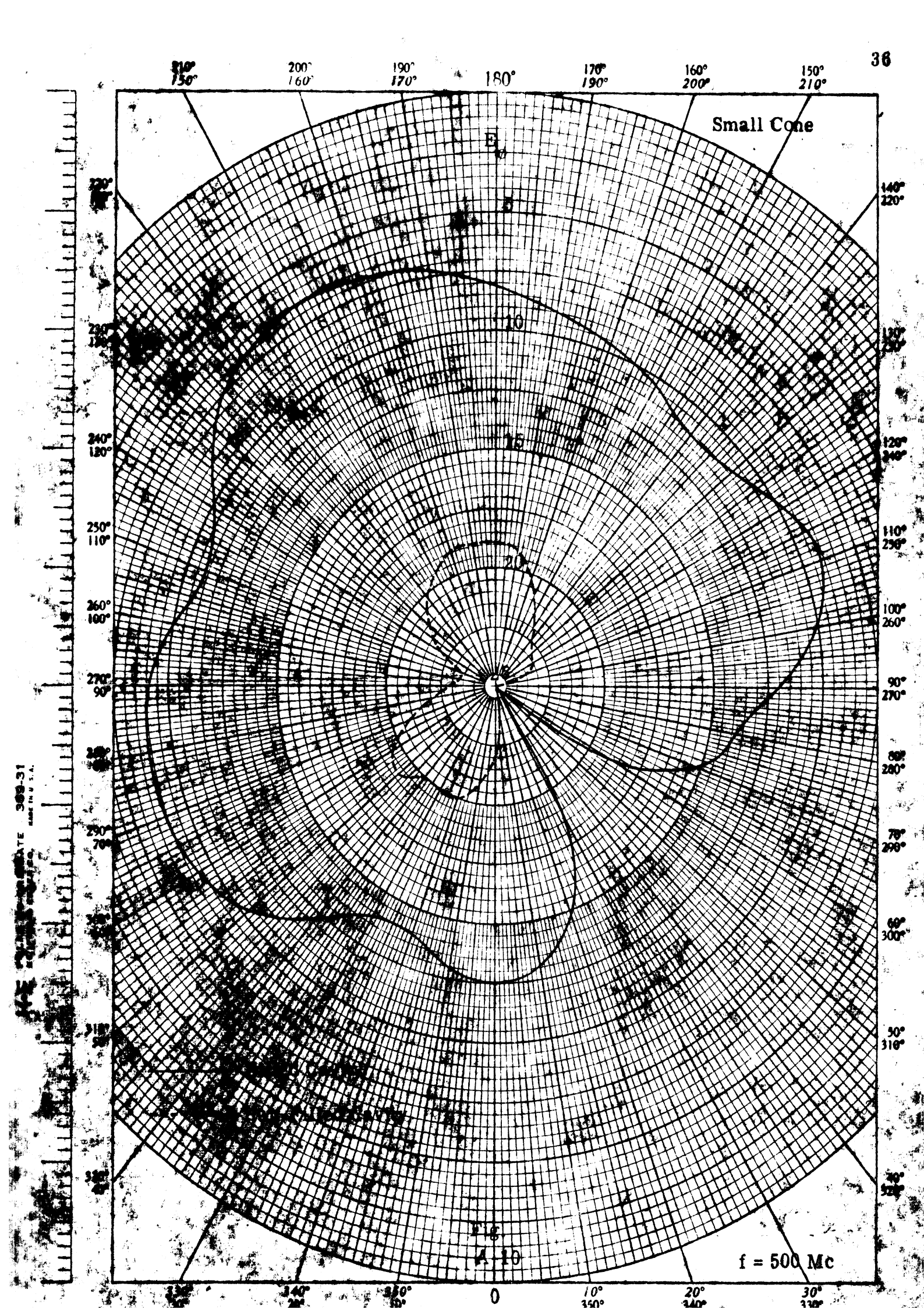

Fig. A-10

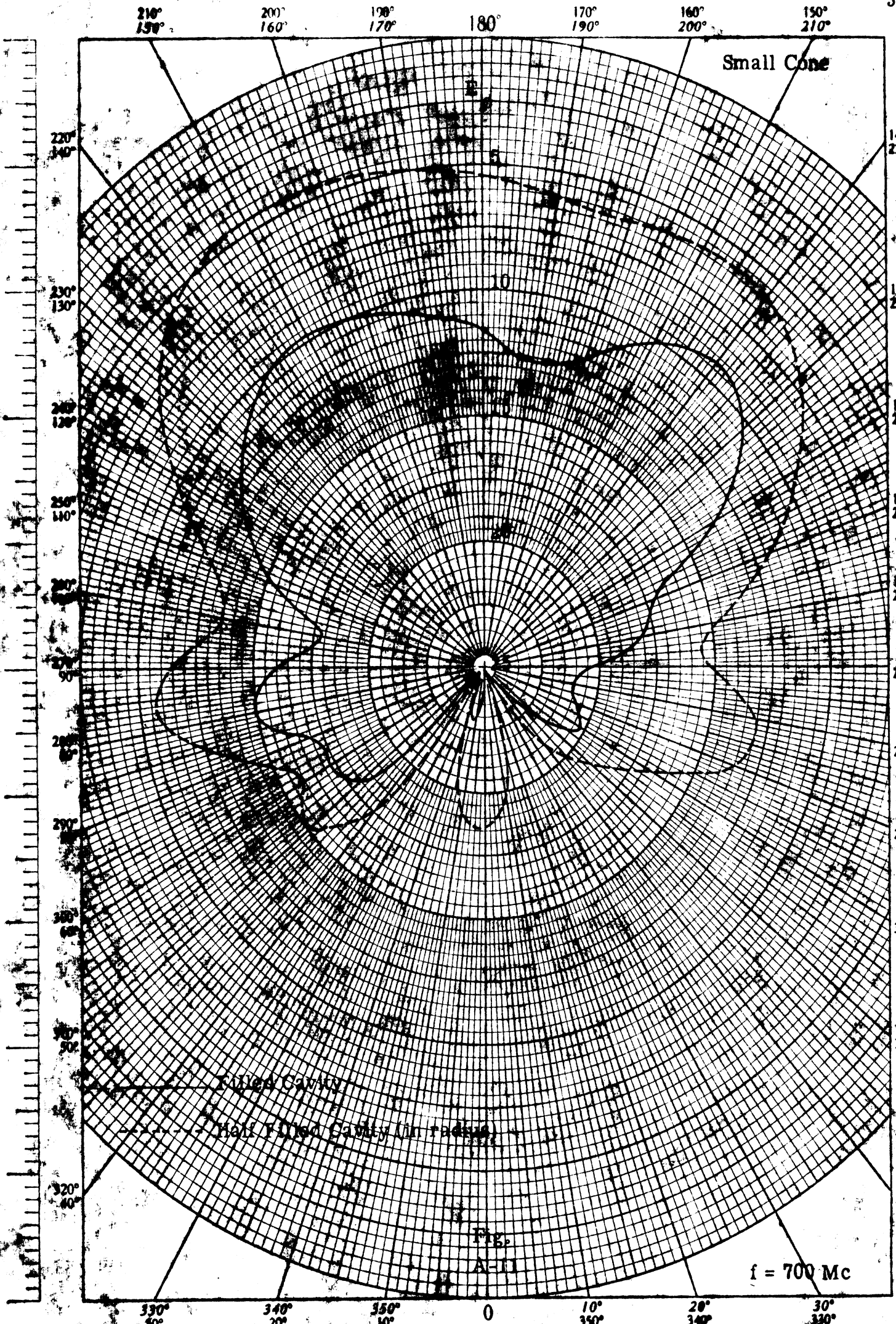
Small Cone
Filled Cavity
Half Filled Cavity (in radius)
f = 700 Mc

Fig. A-11

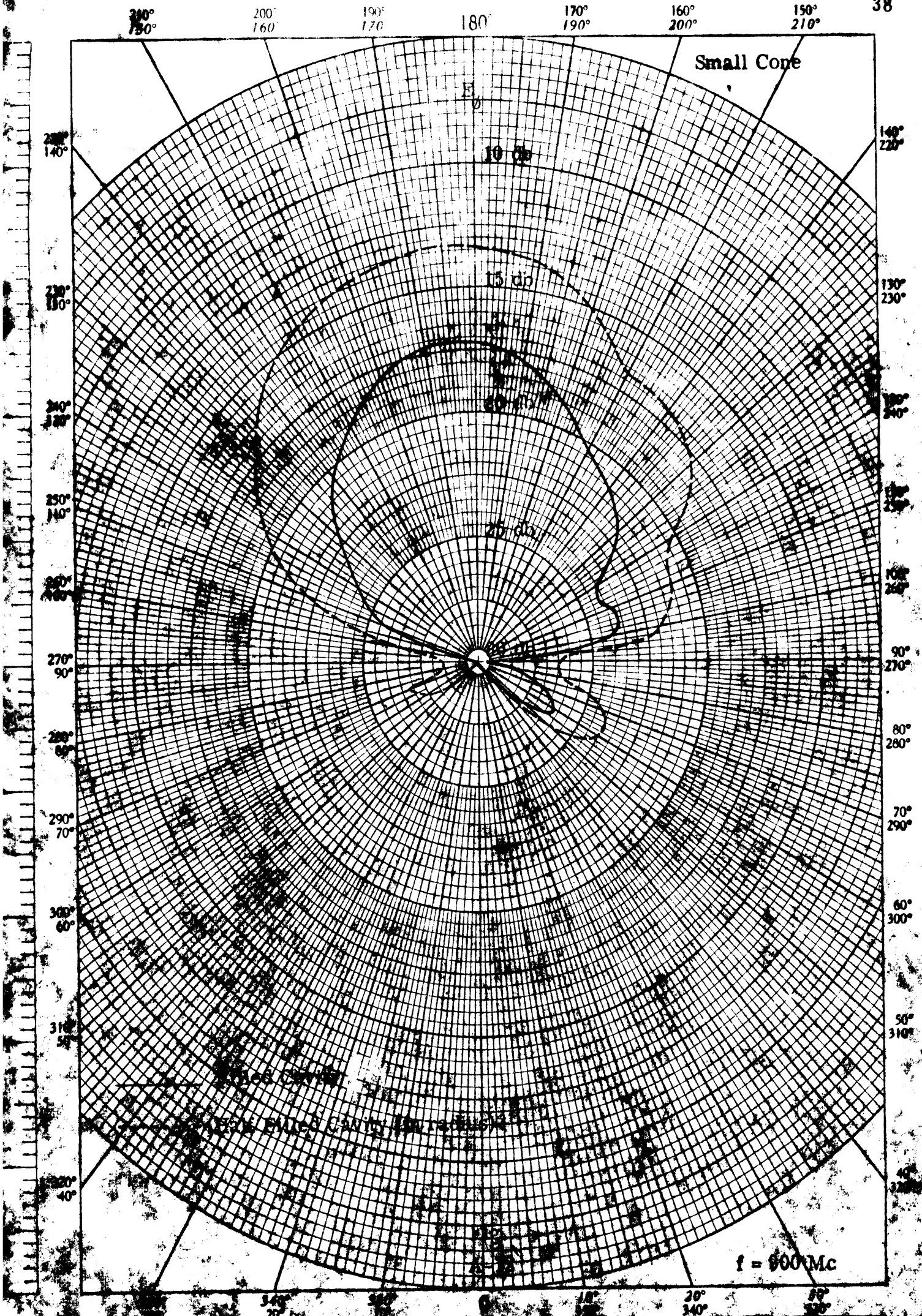
Small Cone
10 db
15 db
20 db
25 db
f = 900 Mc

APPENDIX B

RADIATION PATTERNS FOR THE LARGE LOG CONICAL SPIRAL ANTENNA

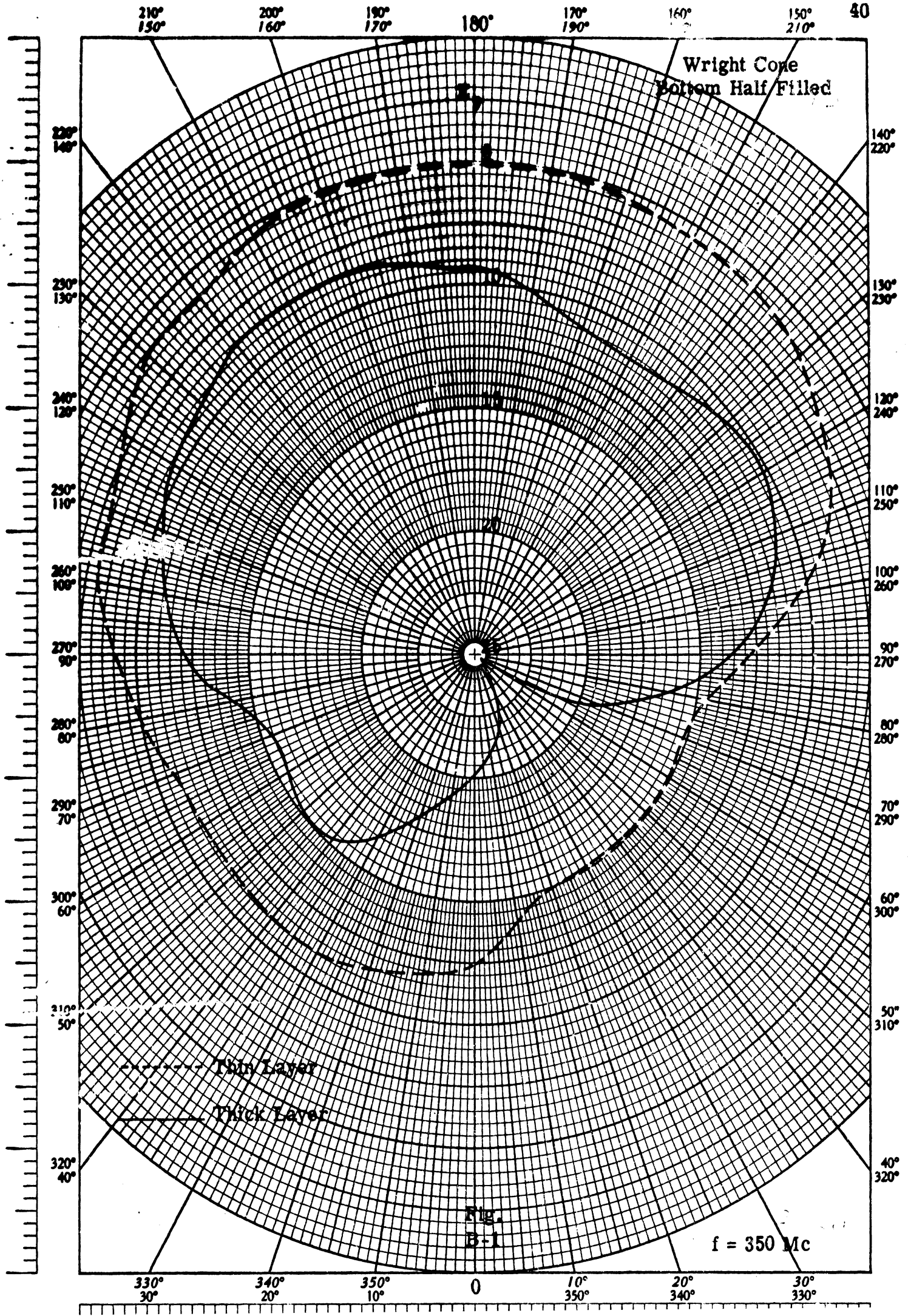
Wright Cone
Bottom Half Filled
Thin Layer
Thick Layer
f = 350 Mc

Fig. B-1

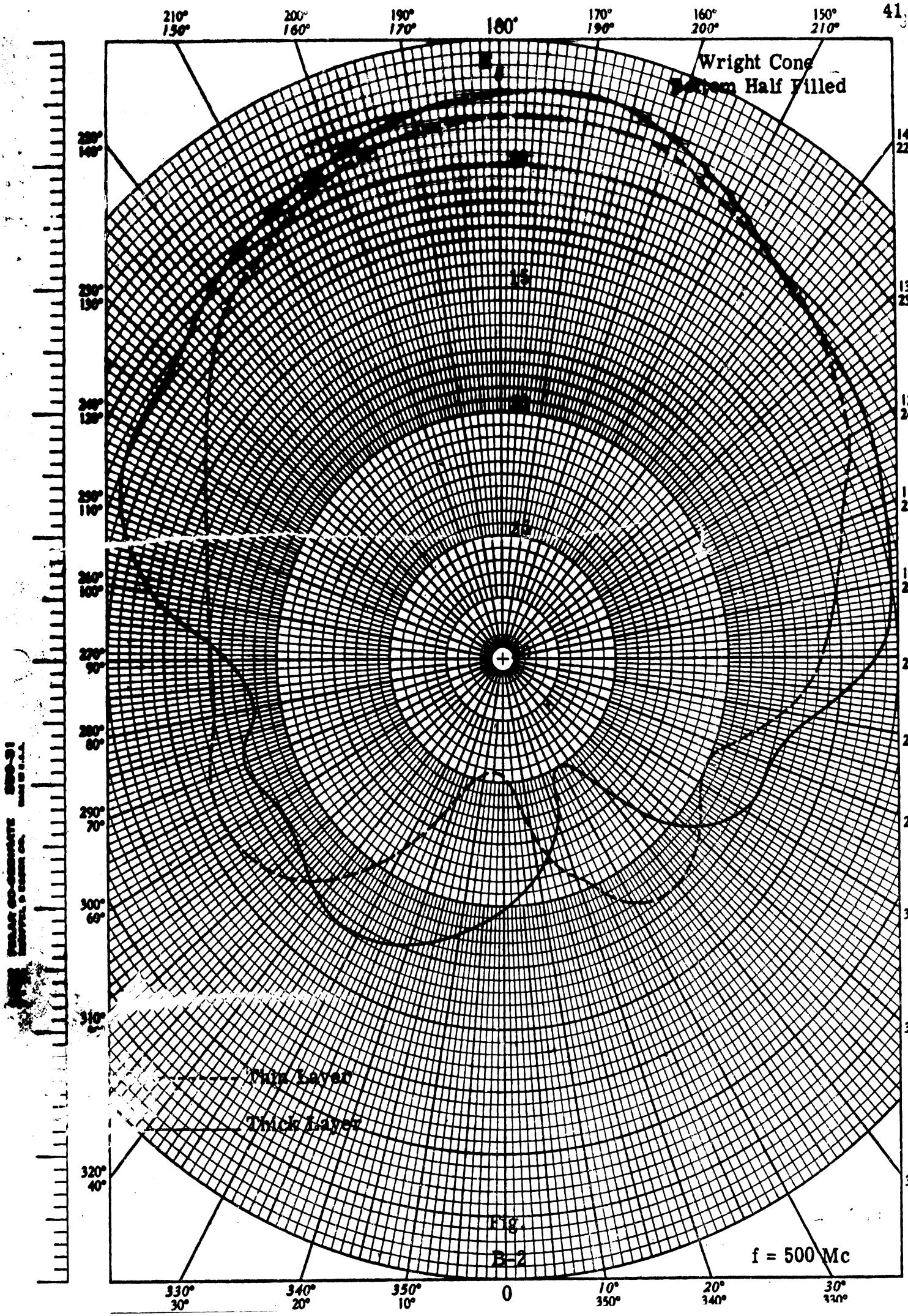
Wright Cone
Bottom Half Filled
Thin Layer
Thick Layer
f = 500 Mc

Fig.
B-2

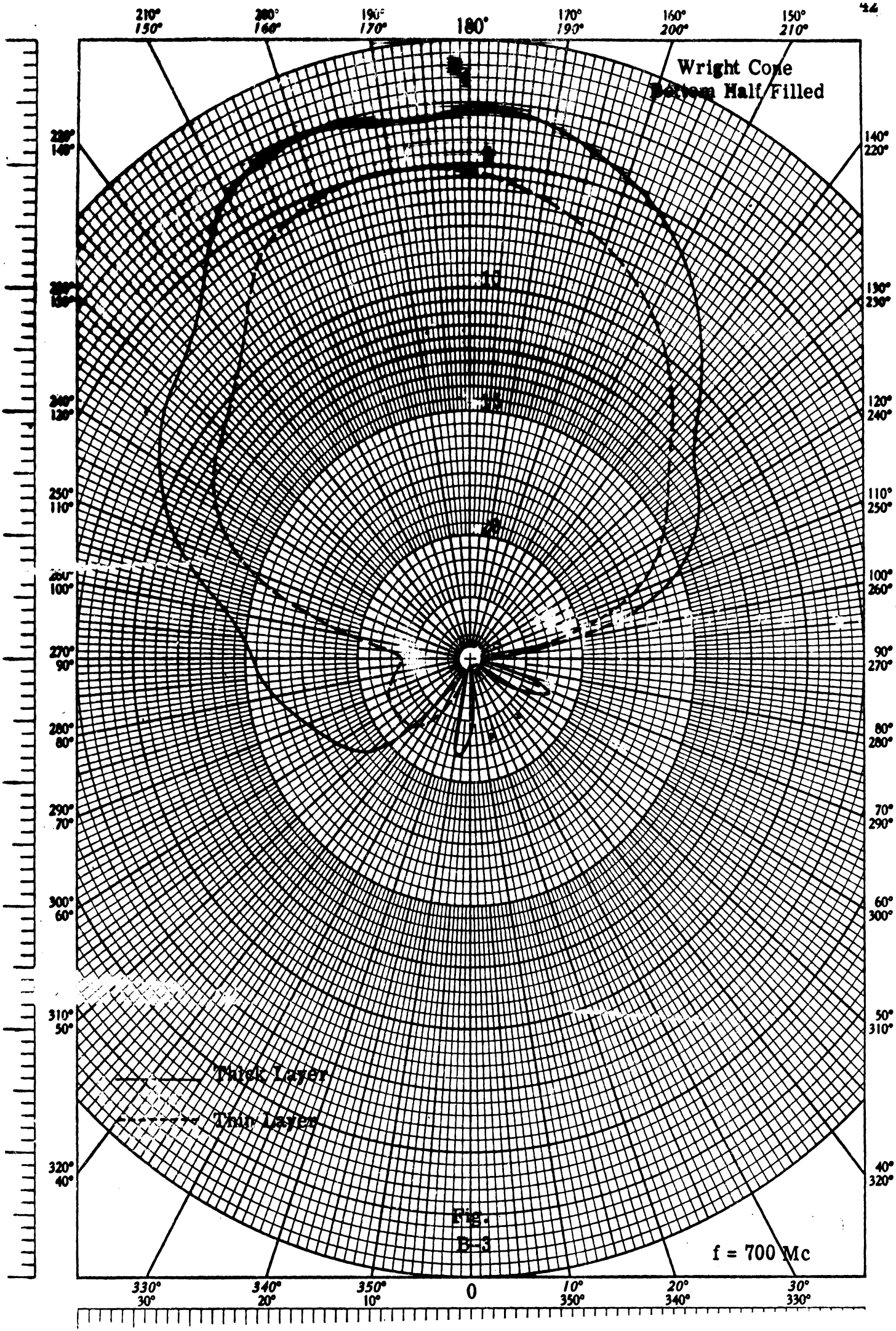
Wright Cone
Bottom Half Filled
Thick Layer
Thin Layer
f = 700 Mc
180°
0
210° 150°
200° 160°
190° 170°
170° 190°
160° 200°
150° 210°
220° 140°
140° 220°
130° 230°
240° 120°
120° 240°
250° 110°
110° 250°
260° 100°
100° 260°
270° 90°
90° 270°
280° 80°
80° 280°
290° 70°
70° 290°
300° 60°
60° 300°
310° 50°
50° 310°
320° 40°
40° 320°
330° 30°
340° 20°
350° 10°
10° 350°
20° 340°
30° 330°

Fig. B-3

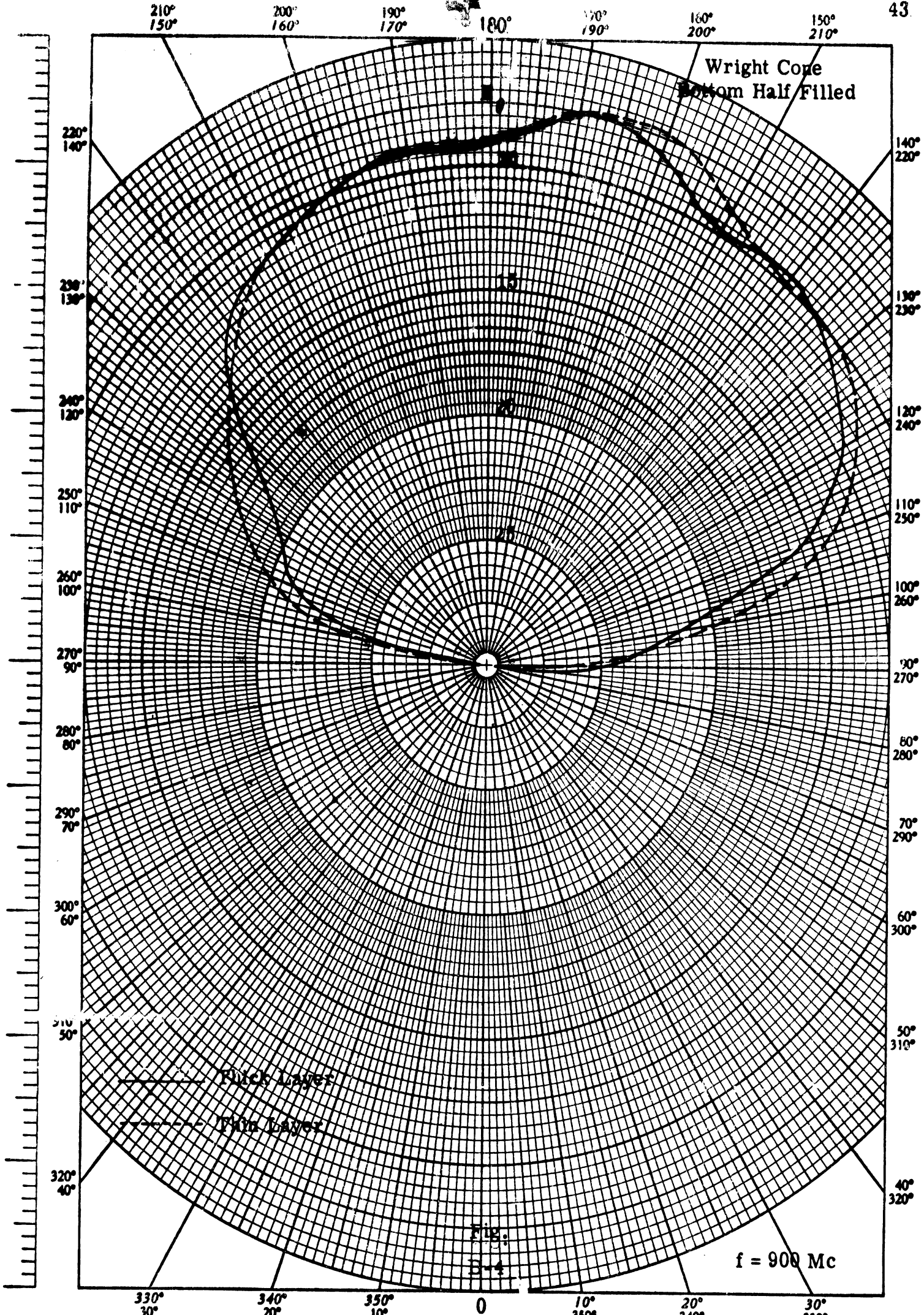
Wright Cone
Bottom Half Filled
Thick Layer
Thin Layer
f = 900 Mc

Fig. 3-4

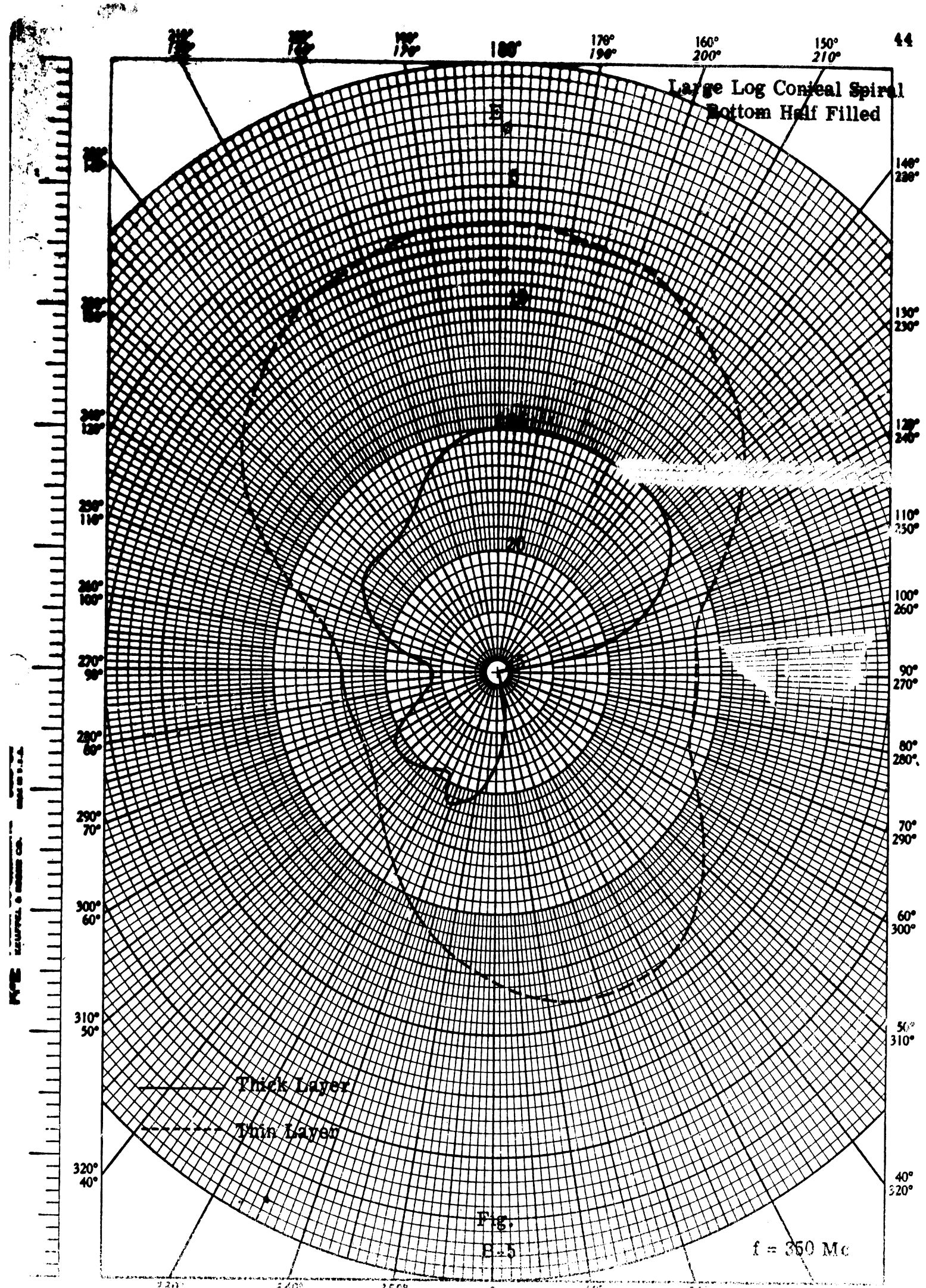

Fig.
E-5

f = 350 Mc

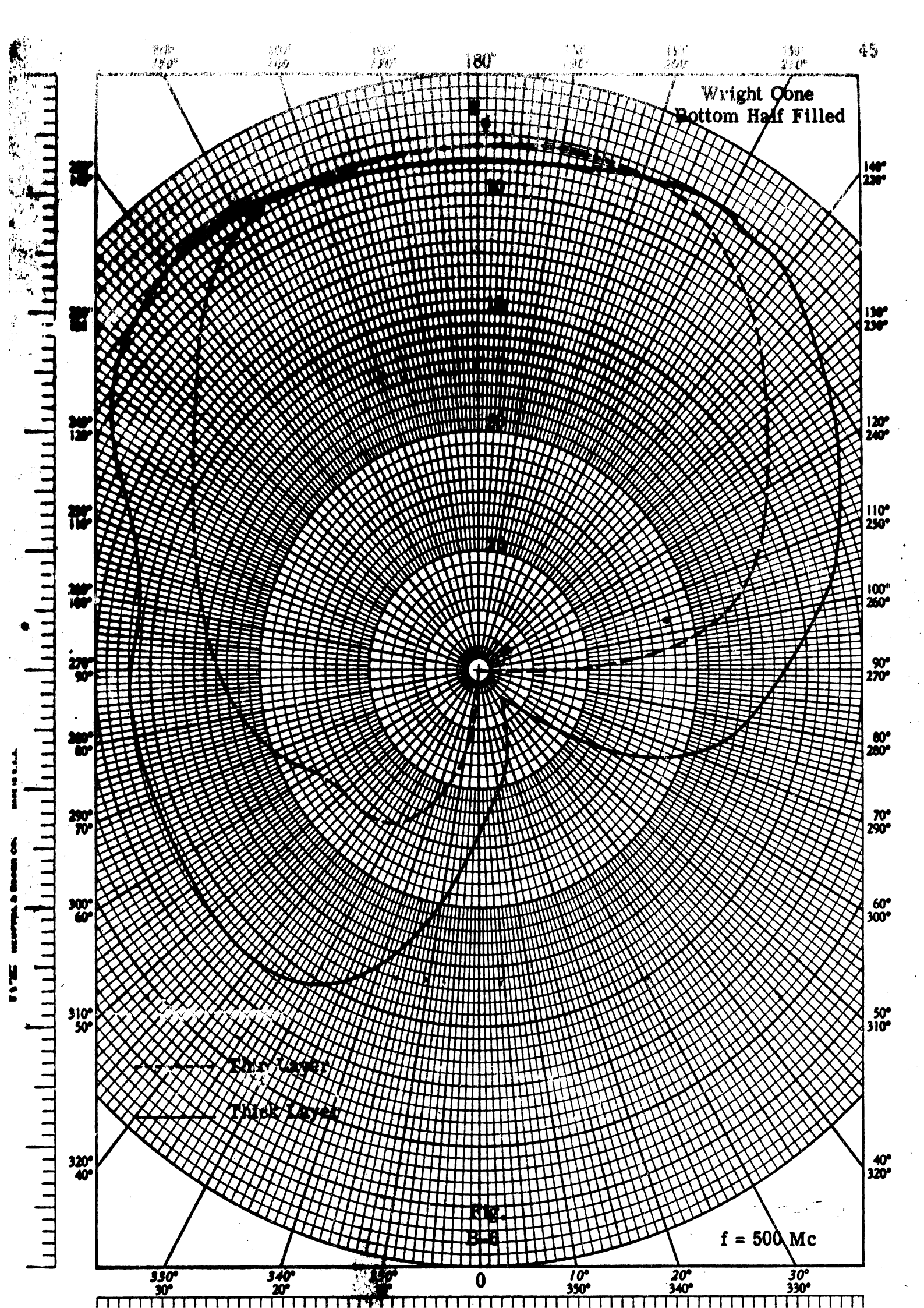
Wright Cone
Bottom Half Filled
Thin Layer
Thick Layer
f = 500 Mc
180°
0
90°
270°

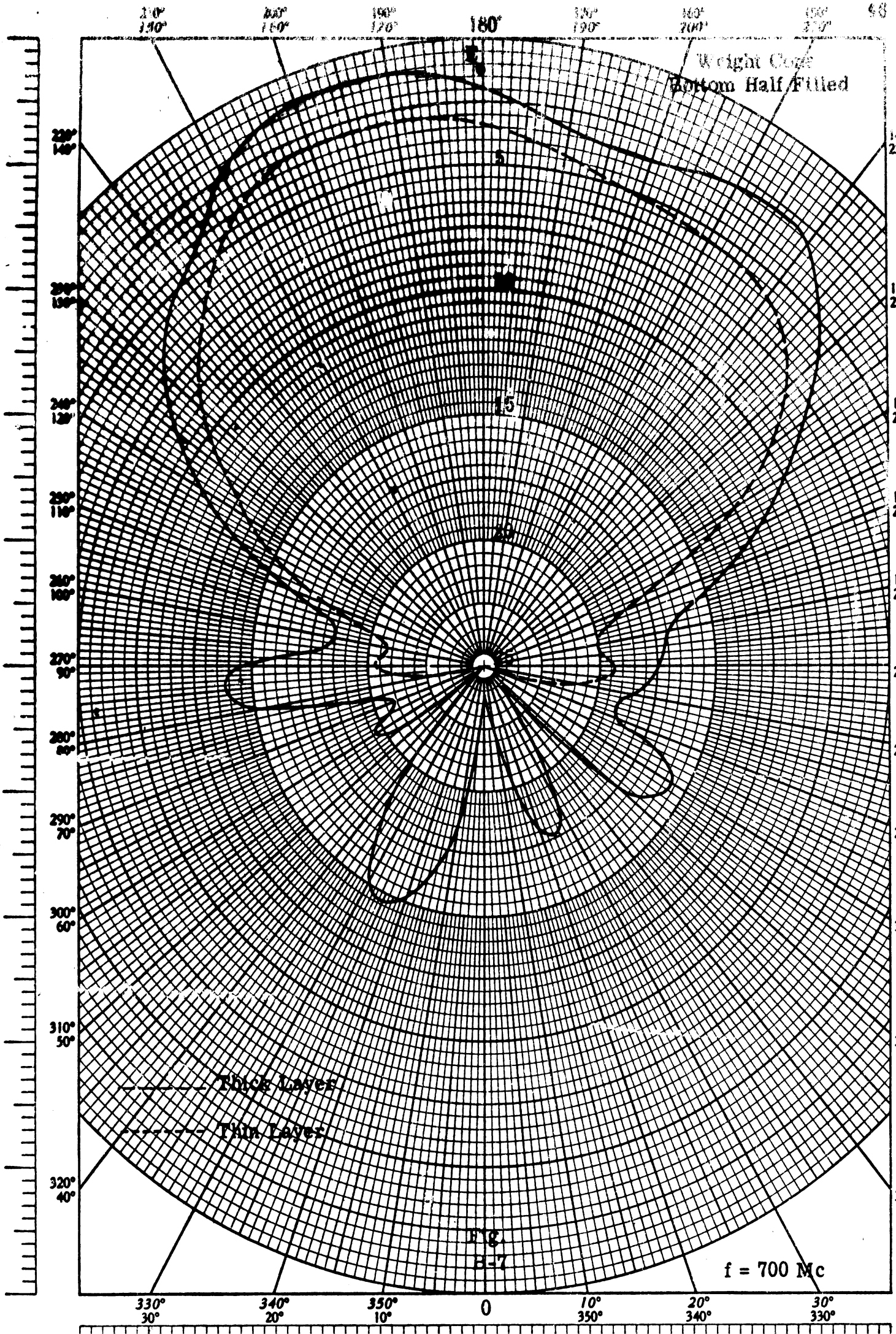
Weight Core
Bottom Half Filled
180°
5
15
20
Thick Layer
Thin Layer
f = 700 Mc
0
330° 30°
340° 20°
350° 10°
10° 350°
20° 340°
30° 330°
220° 140°
230° 130°
240° 120°
250° 110°
260° 100°
270° 90°
280° 80°
290° 70°
300° 60°
310° 50°
320° 40°
140° 220°
130° 230°
120° 240°
110° 250°
100° 260°
90° 270°
80° 280°
70° 290°
60° 300°
50° 310°
40° 320°

Fig. B-7

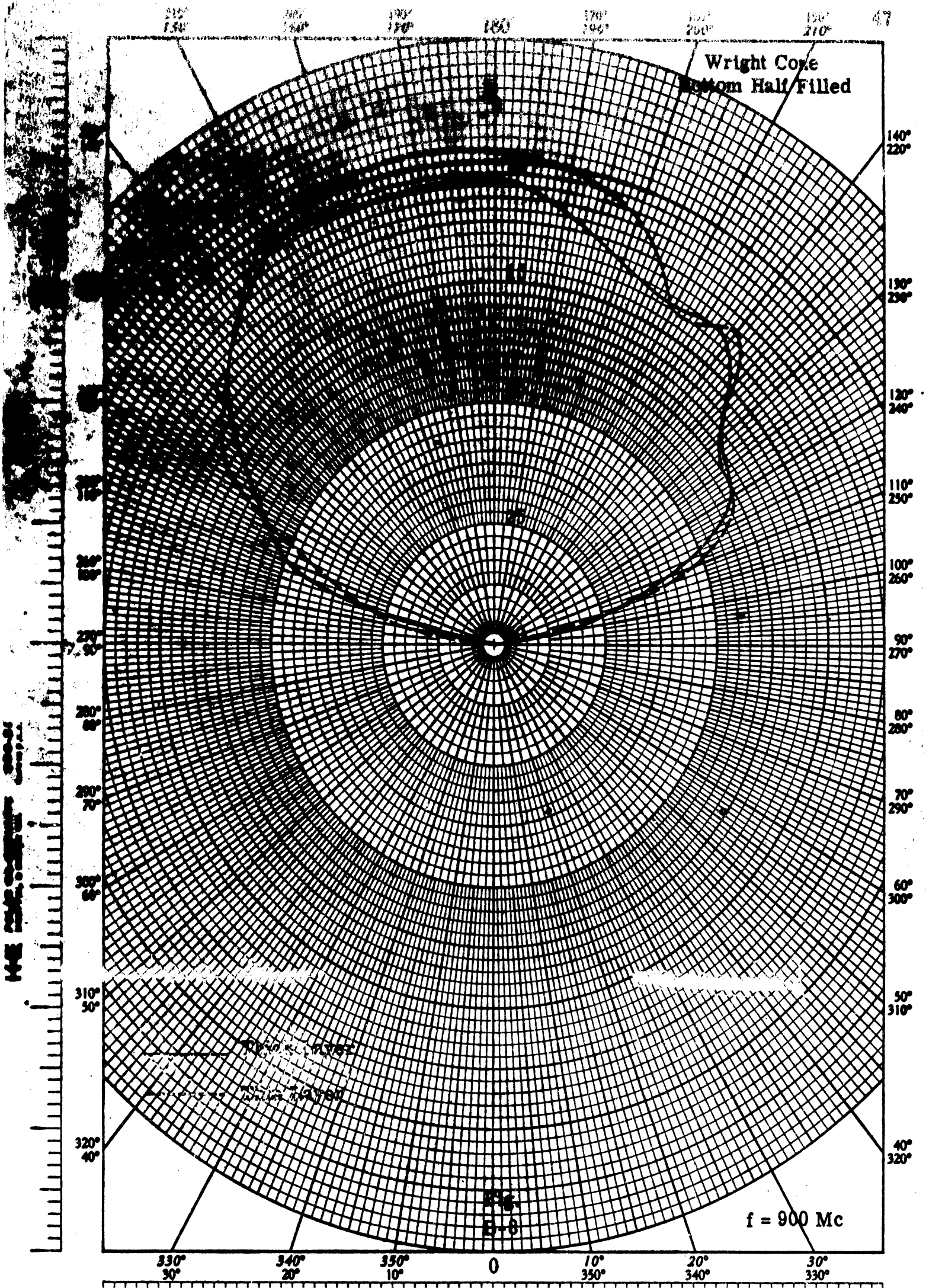
Wright Cone
Bottom Half Filled
f = 900 Mc
0

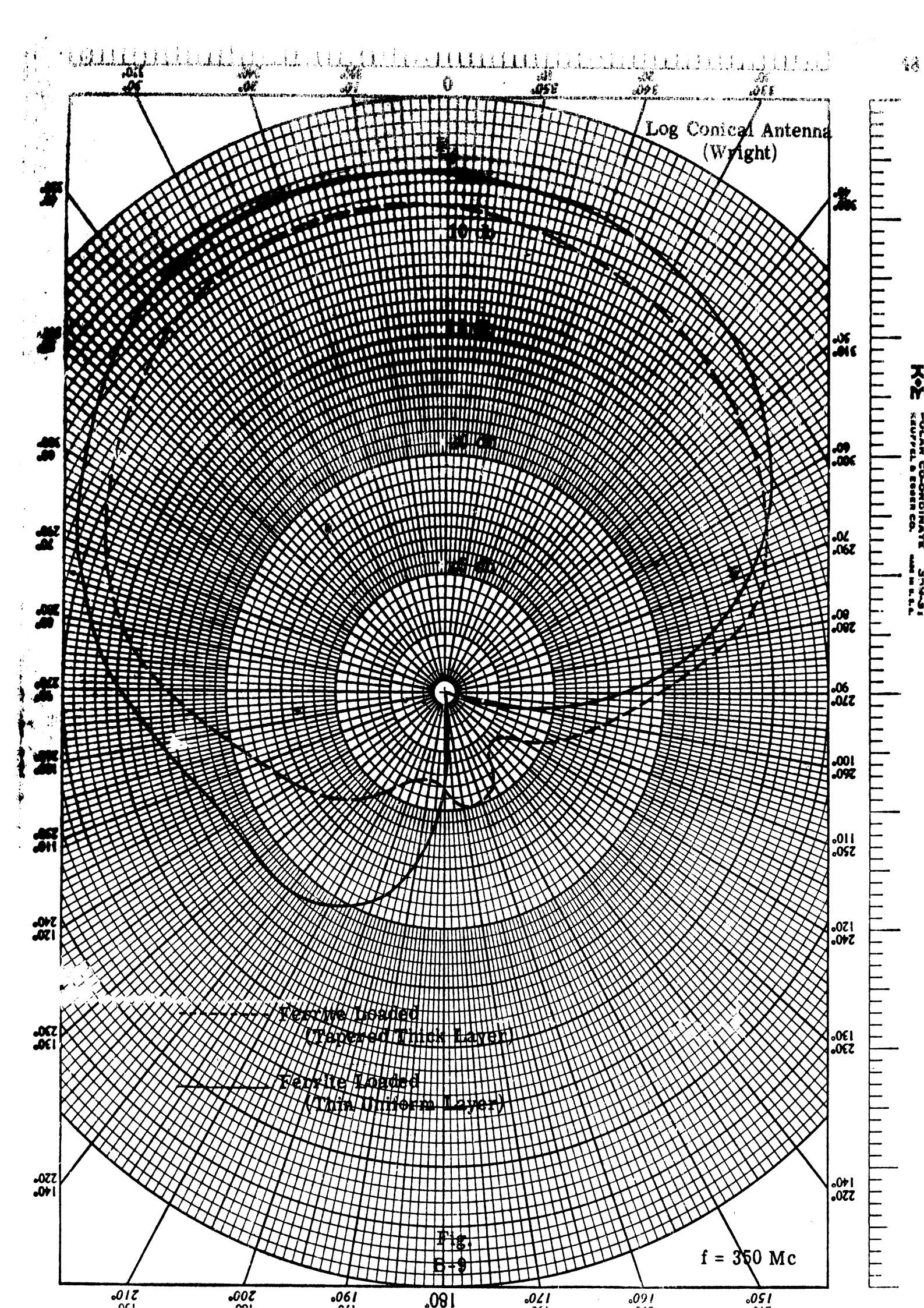
Log Conical Antenna
(Wright)
Ferrite Loaded
(Tapered Thick Layer)
Ferrite Loaded
(Thin Uniform Layer)
f = 350 Mc

Fig. 6-9

Fig.
f = 500 Mc
E=10

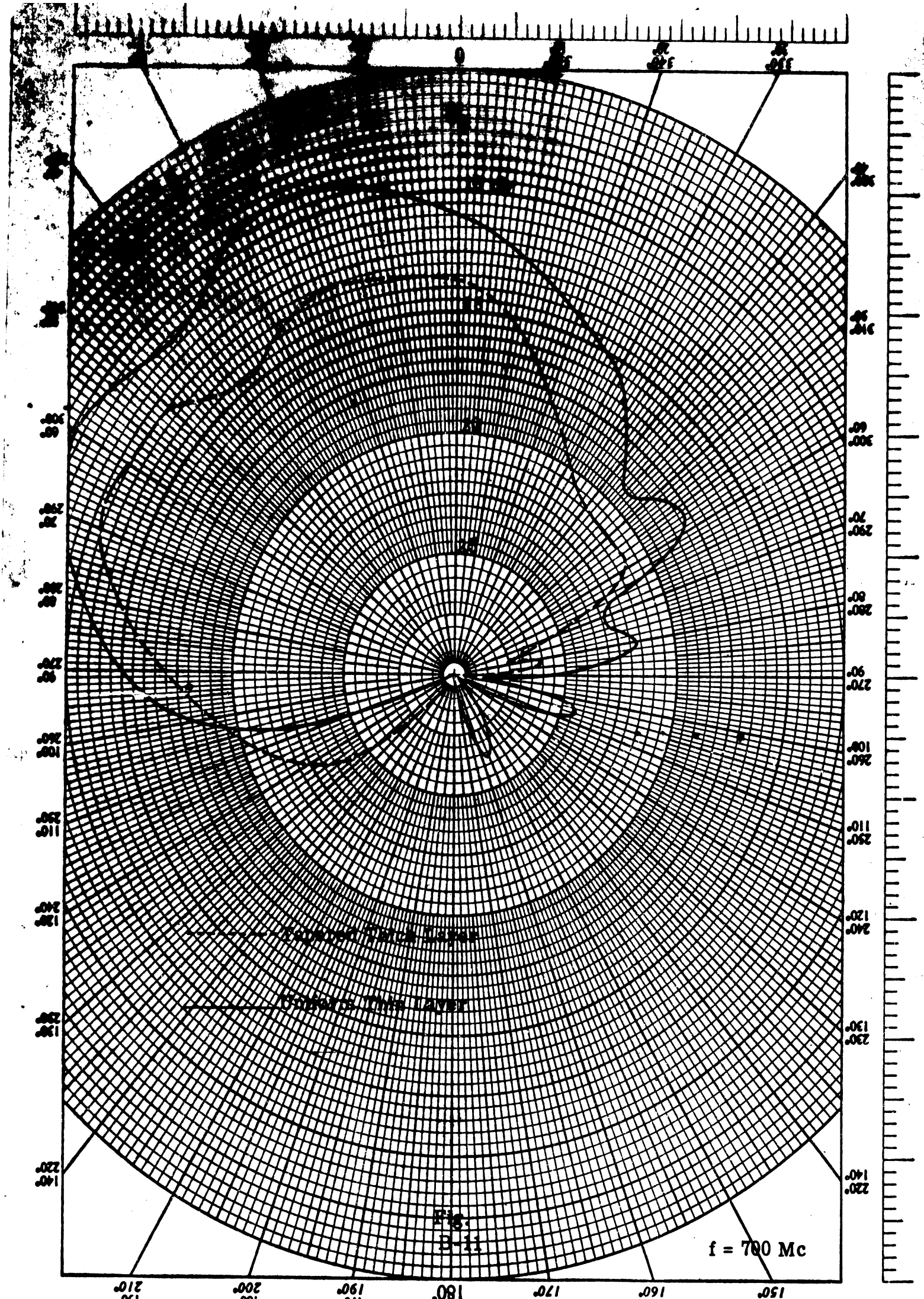
Fig.
D-11
f = 700 Mc

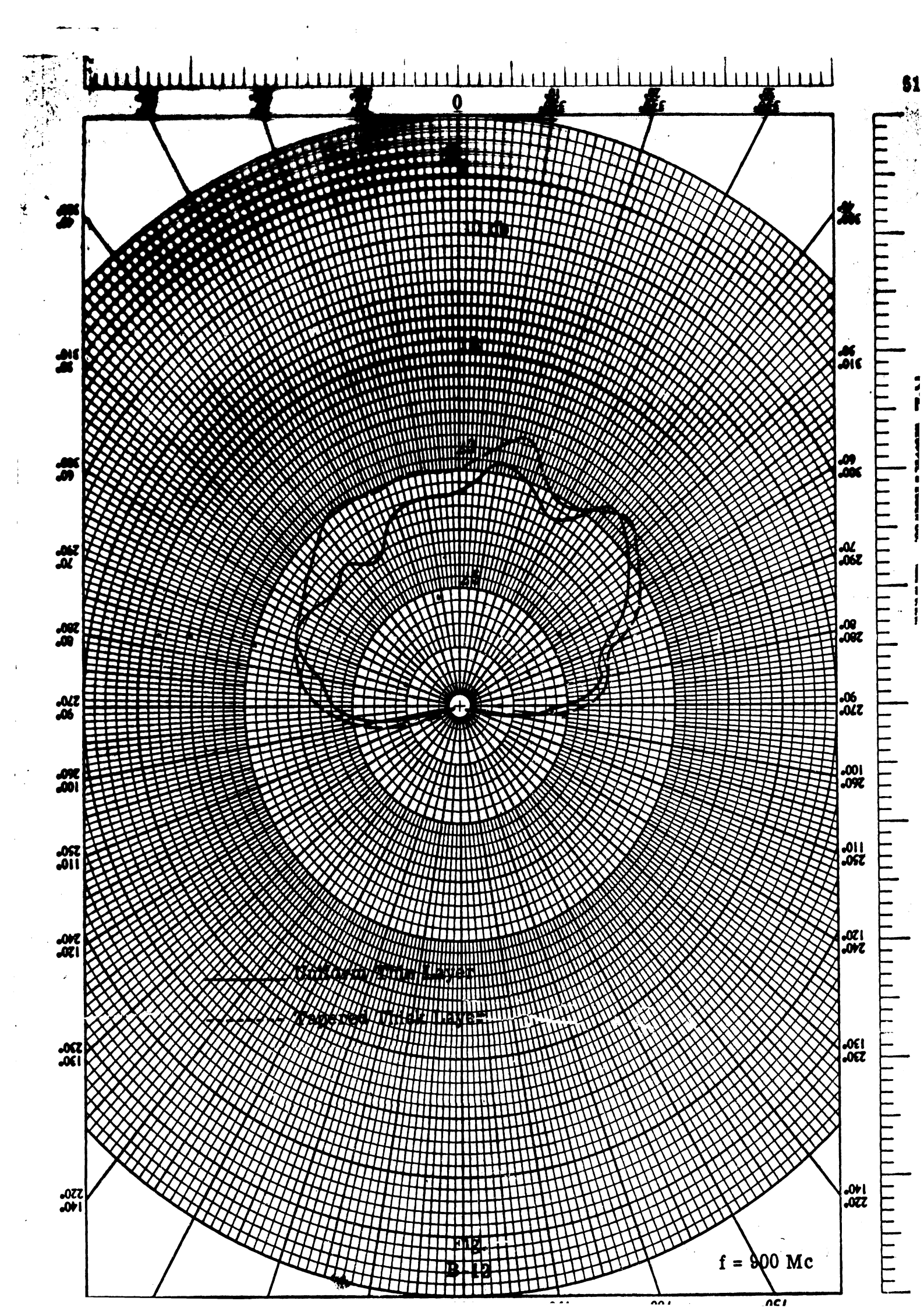

Fig.
B-12

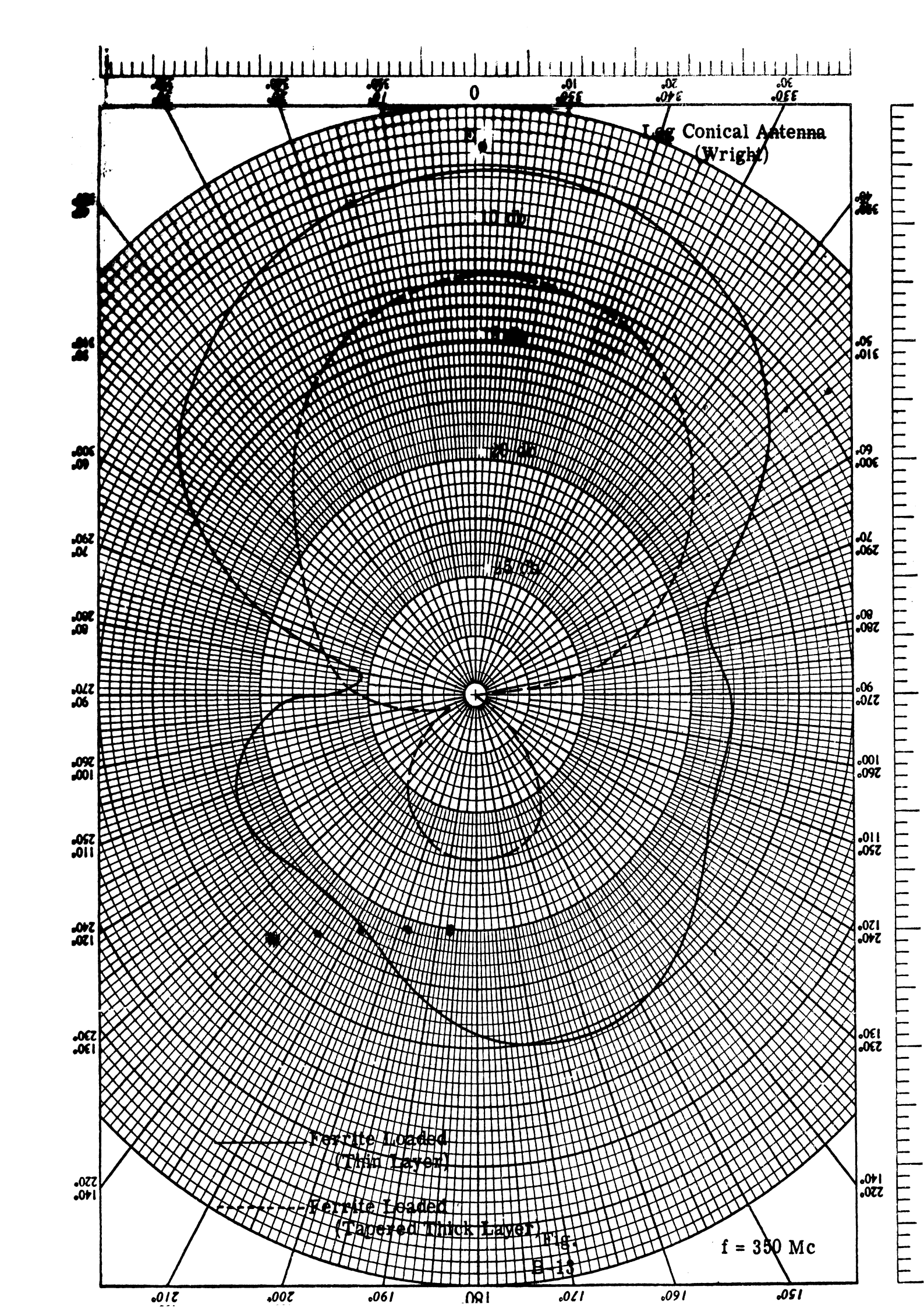
Log Conical Antenna
(Wright)
0
10 db
20 db
25 db
Ferrite Loaded
(Thin Layer)
Ferrite Loaded
(Tapered Thick Layer)
f = 350 Mc

Fig. B-13

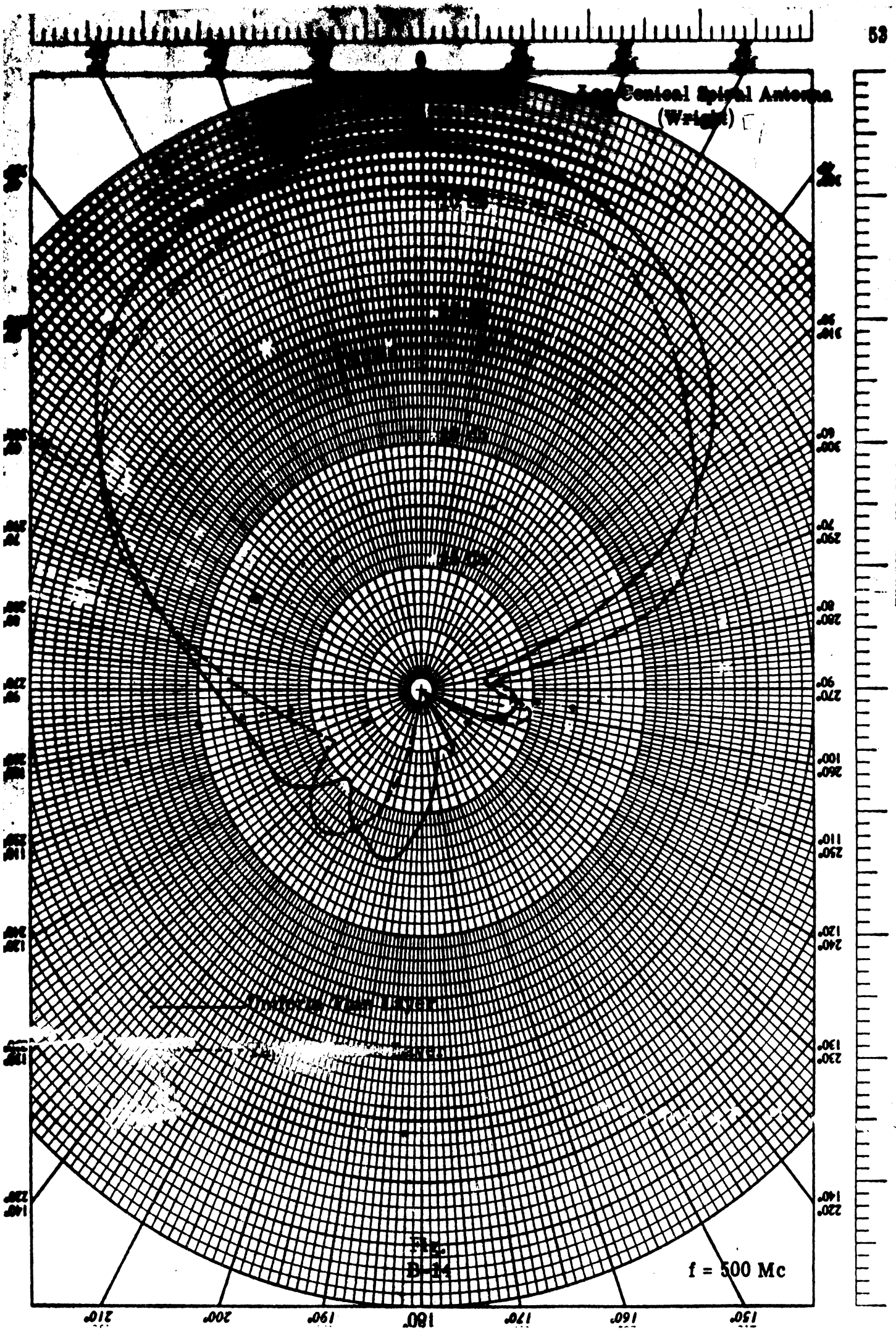

Fig.
B-14

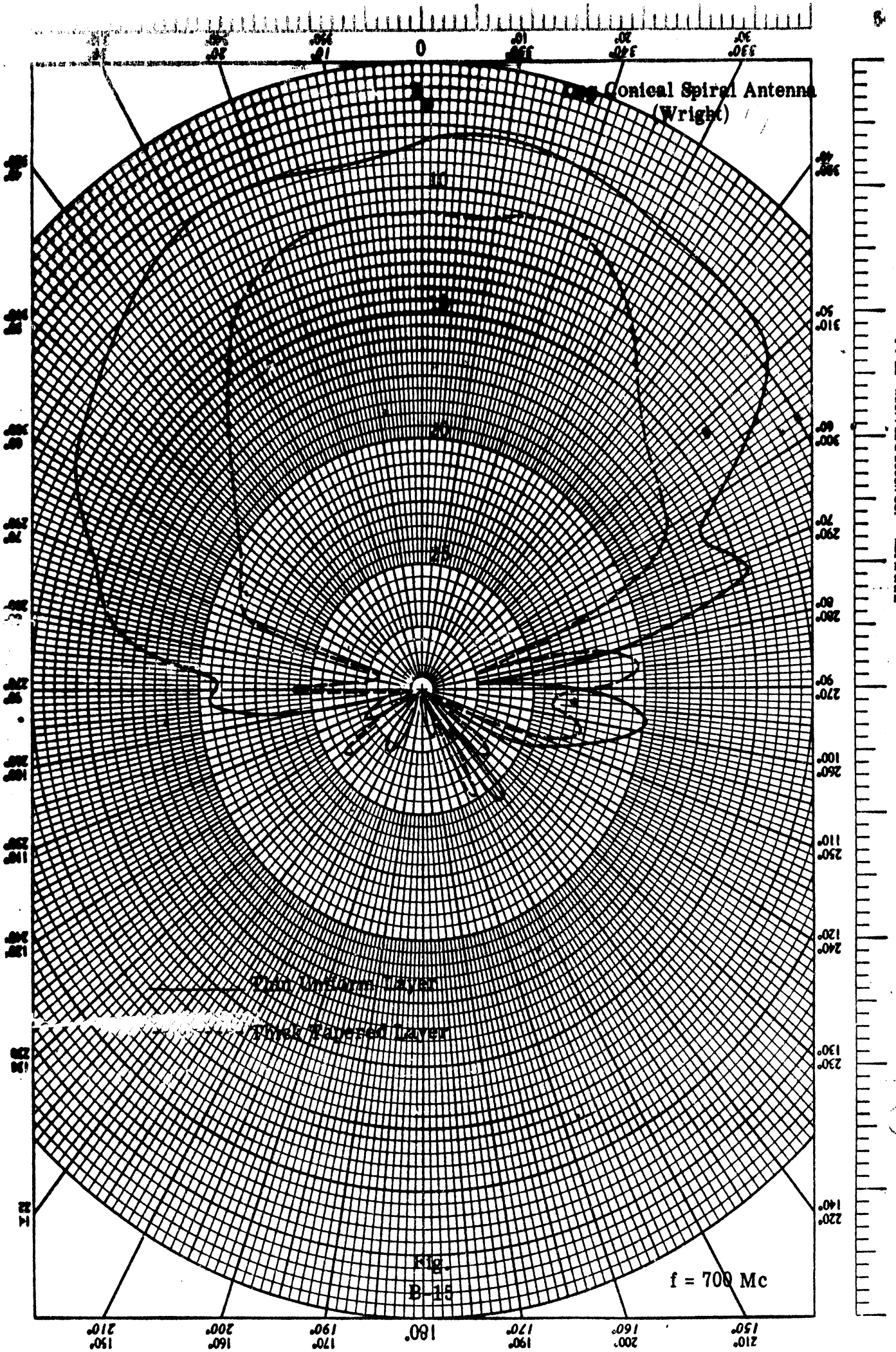
Conical Spiral Antenna
(Wright)
Thin Uniform Layer
Thick Tapered Layer
f = 700 Mc

Fig.
B-15

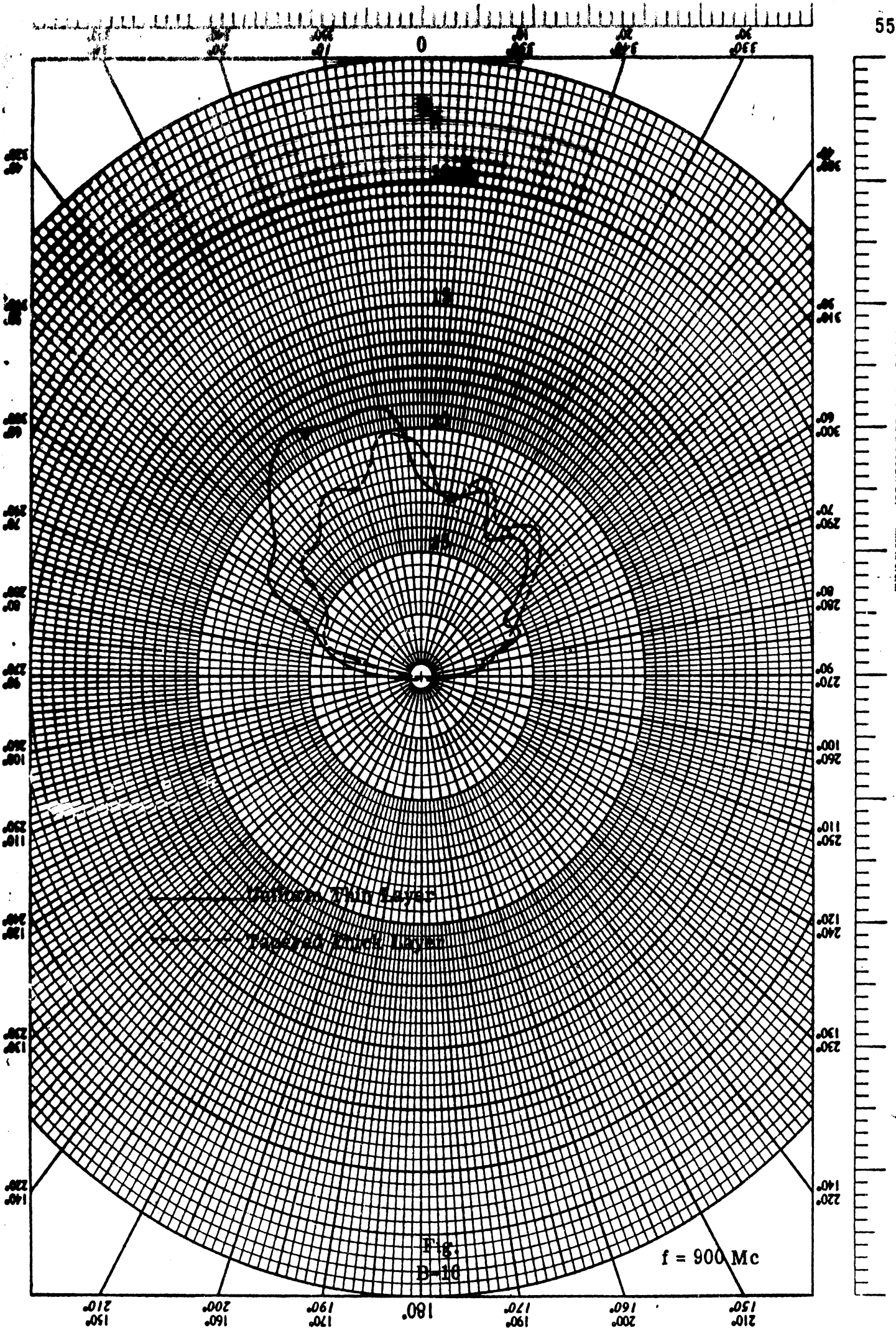
Uniform Thin Layer
Tapered Thick Layer
f = 900 Mc
K+E POLAR CO-ORDINATE 359-31
KEUFFEL & ESSER CO. MADE IN U.S.A.

Fig. B-16